Enhancement of alphavirus replication in mammalian cells at sub-physiological temperatures

Jinchao Guo and Mark Harris*

School of Molecular and Cellular Biology, Faculty of Biological Sciences and Astbury Centre for Structural Molecular Biology, University of Leeds, Leeds, LS2 9JT, United Kingdom.

* Corresponding author, e-mail m.harris@leeds.ac.uk

Word counts: Abstract: 290, author summary: 175, main text: 6656

10 Figures

Keywords: alphavirus; subgenomic replicon; mammalian cells; sub-physiological temperature; stress granules

Short title: Alphavirus replication enhanced at sub-physiological temperatures

Author contributions: JG: conceptualization, formal analysis, investigation, visualization and writing. MH: conceptualization, funding acquisition, supervision, visualization and writing.

Abstract

Chikungunya virus (CHIKV) is a re-emerging Alphavirus transmitted by Aedes mosquitoes and causing fever, rash and arthralgia. Currently there are no vaccines or antiviral agents against CHIKV, therefore it is important to understand the molecular details of CHIKV replication. In this regard, the function of the Alphavirus non-structural protein 3 (nsP3) remains enigmatic. Building on previous studies (Gao *et al*, 2019), we generated a panel of mutants in a conserved and surface exposed cluster in the nsP3 alphavirus unique domain (AUD) and tested their replication phenotype using a sub-genomic replicon (SGR) in mammalian and mosquito cells. We identified three mutants that replicated poorly in mammalian cells but showed no defect in mosquito cells. We further showed that these mutants were temperature-sensitive, rather than species-specific, as they exhibited no replication defect in mammalian cells at sub-physiological temperature (28°C). Similar effects were observed in the context of infectious CHIKV as well as a closely related virus: O'Nyong Nyong virus (ONNV). Intriguingly, this analysis also revealed that the wildtype SGR replicated much more efficiently at sub-physiological temperature as compared to 37°C. This was not due to impaired interferon responses as this enhancement was also observed in Vero cells. Neither was this due to a defect in the phosphorylation of eIF2α as treatment with ISRIB, an inhibitor of global translation attenuation, did not compensate for replication defects at 37°C. However, we noticed significant differences between the sizes and numbers of virus-induced stress granules (SG) at physiological and sub-physiological temperatures. As cells in the periphery will be at sub-physiological temperatures, and these will be the first cells infected in the

mammalian host following a mosquito bite, we propose that alphaviruses have evolved mechanisms to limit antiviral responses in these cells to promote viral genome replication.

Author summary

Chikungunya virus (CHIKV) is a re-emerging arbovirus. It is transmitted by *Aedes* species of mosquitos and poses massive epidemic threats. Arboviruses are unique in that they must be able to replicate efficiently in both the mosquito vector and the mammalian host, and therefore at different temperatures. Importantly, the first cells infected in the mammalian host following a mosquito bite will be in the skin and therefore at sub-physiological temperature (lower than 37°C). Here we show that mutants within one of the CHIKV proteins (nsP3) were unable to replicate at 37°C but replicated efficiently in mammalian cells at a sub-physiological temperature (28°C). We also showed that the wildtype virus replicated more efficiently at 28°C in comparison to at 37°C in mammalian cells. We investigated the mechanism behind this phenomenon and showed that at sub-physiological temperatures the virus induced the formation of smaller and more numerous cytoplasmic stress granules. We propose that alphaviruses have evolved mechanisms to promote their replication in mammalian cells at sub-physiological temperatures to facilitate infection of mammals via a cutaneous mosquito bite.

58 # Introduction

59 Chikungunya virus (CHIKV) belongs to the *alphavirus* genus in the *Togaviridae* family [1].
60 It is an arbovirus that is transmitted by mosquitoes and causes fever, rash and arthralgia
61 with infrequent long-term morbidity and in rare cases mortality [2]. CHIKV was first
62 isolated in Tanzania in 1952-1953 [3, 4], and has subsequently spread across the world,
63 including Africa, Europe, Asia and America [5, 6]. CHIKV is mainly transmitted by the
64 mosquito species *Aedes aegypti* and *Ae. albopictus*, the latter has become the main
65 vector for virus spread in Asia [7]. Both field and laboratory experiments demonstrated
66 that the survival rate of these two mosquito species are affected by lower and upper
67 temperature thresholds [8]. Models and human cases showed transmission occurs
68 between 18°C and 34°C with maximal transmission occurring in a range from 26-29°C
69 [9].

70 CHIKV has a positive-sense, single-stranded RNA genome, 11.5 kb in length, which is
71 both capped and polyadenylated (Fig 1A). It contains two open reading frames (ORFs),
72 the first ORF encodes the non-structural proteins (nsP1-nsP4) and is translated directly
73 from full-length genomic RNA. ORF2 encodes the structural proteins (Capsid, E1-E3 and
74 6K) and is translated from a sub-genomic RNA. nsP1 to nsP4 are required for the
75 synthesis of positive and negative full-length genomic RNA as well as the sub-genomic
76 RNA. Biochemical analysis indicated specific functions of the non-structural proteins:
77 nsP1 shows methyl-and guanyl-transferase activities, nsP2 exhibits helicase and
78 protease activities, nsP4 is the RNA-dependent RNA polymerase. The function of nsP3
79 remains poorly defined [10], although it is essential in genome replication. CHIKV nsP3
80 consists of three domains: a macro-domain at the N-terminus, the central alphavirus

81 unique domain (AUD) and the hypervariable domain (HVD) at the C-terminus (Fig 1A).
82 The macro-domain exhibits RNA binding, ADP-ribose binding and ADP-ribosylhydrolase
83 activities [11-13]. The HVD is highly phosphorylated and interacts with a number of host
84 proteins [14]. Despite high levels of conservation across alphaviruses, AUD function
85 remains elusive. In this context our recent work showed that the AUD binds to viral RNA
86 and plays a role in virus assembly by stimulating production of the sub-genomic RNA [15].

87 Eukaryotic initiation factor 2 (eIF2) is a key regulator of protein synthesis in mammalian
88 cells [16]. Phosphorylation of the eIF2 α-subunit by one of four kinases (HRI, GCN2, PKR
89 and PERK) prevents guanine nucleotide exchange on eIF2 and the regeneration of the
90 active GTP-bound state, resulting in global translation attenuation [17]. Most
91 alphaviruses possess a translation enhancer element within the sub-genomic RNA open
92 reading frame that has been shown to counteract the translational inhibition in the
93 presence of high levels of eIF2α phosphorylation [22, 23]. Although CHIKV does not
94 contain this element, CHIKV nsP4 has been shown to suppress eIF2α phosphorylation
95 [24].

96 Translation attenuation via eIF2α phosphorylation results in the accumulation of stalled
97 48S mRNPs into cytoplasmic, non-membranous aggregates termed stress granules (SG).
98 Typical SG contain silent mRNAs, translation factors, small ribosomal subunits, and
99 various mRNA-binding proteins. Despite varied compositions resulting from different
100 stresses [25], certain components including the Ras GTP-activating protein-binding
101 protein G3BP1/2, are required for formation of all SGs [26, 27]. Alphavirus infection
102 induces SG formation during the early stages [28]. It is assumed that upon virus-induced
103 stress, 48S mRNPs bound by G3BP1 and other components such as TIA-1 form small

104 core aggregates that grow into larger SGs [29]. SG are highly dynamic and exhibit rapid
105 exchange of mRNPs [30]. They can grow to several μm in diameter in 20 min and can
106 be disassembled completely within 60 mins following the cessation of environmental
107 stress or the addition of polysome-stabilizing agents such as cycloheximide (CHX) [31].
108 The CHIKV nsP3 hypervariable domain has been shown to interact with G3BP1/2 and
109 regulate their localization [32]. Recent work demonstrated that the composition and
110 disassembly of SG was determined by the ADP-ribosylhydrolase activity within the CHIKV
111 nsP3 macro-domain [33].

112 In this study we sought to investigate the function of AUD in CHIKV replication in cells
113 from both the vertebrate host and the mosquito vector. Three AUD mutants (W220A,
114 D249A and Y324A) replicated poorly in mammalian cells but efficiently in mosquito cells,
115 and we demonstrate that this phenotype was temperature-dependent rather than species-
116 specific. Importantly, we also demonstrated that a wildtype CHIKV sub-genomic replicon
117 (SGR) replicated more efficiently in mammalian cells at a sub-physiological temperature.
118 Although phosphorylation of eIF2α was suppressed at lower temperature, it was not the
119 key factor regulating the replication phenotypes observed. Using the related O'Nyong
120 Nyong virus (ONNV) we revealed that at sub-physiological temperatures formation of SG
121 in response to infection was altered. This provided a potential explanation for the
122 enhanced genome replication at sub-physiological temperature.

123

124 # Results

125 ## Construction and analysis of the AUD mutants

126 To identify conserved residues within the CHIKV AUD across the *Alphavirus* genus, a
127 variety of AUD amino acid sequences from both Old and New World alphaviruses were
128 aligned (S1A Fig). As the nsP2/nsP3 protein structure of Sindbis virus (SINV) has been
129 determined [34], and the AUD sequences between SINV and CHIKV share high
130 homology (118 out of 243 residues are identical), a panel of conserved and surface
131 exposed residues in the AUD were selected for mutation based on the SINV nsP2/nsP3
132 protein structure [34] (Fig 1B and S1B Fig). Seven residues were chosen for further study
133 as they were absolutely conserved or in other cases substituted by residues with similar
134 physical characteristics. Y324 (nsP3 amino acid numbering) was selected as a control
135 as it is located at the end of AUD and conserved among alphaviruses. These mutations
136 were introduced into a CHIKV dual luciferase sub-genomic replicon (SGR-D-Luc) (Fig 1A),
137 which was derived from the ECSA strain LR2006 OPY1 isolate [35, 36]. In this construct
138 renilla luciferase (R-Luc) is fused within the nsP3 hypervariable domain in ORF1, and
139 firefly luciferase (FF-Luc) replaces the structural proteins in ORF2. The activity of R-Luc
140 is thus a marker of ORF1 translation from the full-length RNA: at early time points R-Luc
141 levels reflect transfection efficiency and input RNA translation, at later times R-Luc is also
142 dependent upon genome replication. As ORF2 is translated from a sub-genomic RNA
143 (sgRNA) which is templated from the negative strand replicative intermediate, FF-Luc
144 expression is dependent upon genomic replication but will also reflect translation from the

145 sgRNA. A polymerase-inactive mutant (GDD-GAA in nsP4) was used as a negative
146 control.

147 The AUD mutants in SGR-D-Luc exhibited different replication 148 phenotypes in mammalian and mosquito cells

149 CHIKV mainly induces arthritis and joint pain [2] and infects muscle cells. We therefore
150 chose to investigate the effects of the AUD mutants on CHIKV genome replication initially
151 in C2C12, an immortalized mouse myoblast cell line widely used in the study of CHIKV
152 [37]. As expected, wildtype (WT) SGR-D-Luc showed a very high level of replication in
153 C2C12 cells, with FF-Luc levels peaking at 12 h post transfection (h.p.t) and increasing
154 over 1000-fold between 4-12 h.p.t. (Fig 2A). AUD mutants T218A, M219Q, P221A,
155 C246A and A251Q exhibited similar levels of replication as compared to WT, however,
156 W220A, D249A and Y324A showed significant lower levels of replication compared to
157 WT (Fig 2A).

158 As CHIKV is transmitted by mosquitoes we then evaluated the replication capacities of
159 the AUD mutants in C6/36 and U4.4 cells, both derived from *Ae. albopictus* mosquitoes.
160 Importantly, C6/36 cells harbor a frameshift mutation in the Dicer-2 (Dcr2) gene, which
161 leads to the translation of a truncated Dcr2 protein and a defect in the RNAi response
162 [38]. Consistent with this, although WT SGR-D-Luc showed robust replication in both cell
163 lines, C6/36 supported higher levels of replication than U4.4 cells (Fig 2B). Interestingly,
164 unlike the replication defects observed in C2C12 cells, all AUD mutants showed similar
165 levels of replication compared to WT in both U4.4 and C6/36 cells (Fig 2B).

166 The striking phenotypic differences between mammalian and mosquito cell lines for the
167 three AUD mutants (W220A, D249A and Y324A) led us to investigate further. A simple
168 explanation might be that these mutants had reverted to WT in mosquito cells as we had
169 previously observed this for the AUD mutant R243A/K245A [15]. This mutant replicated
170 poorly in mammalian cells but efficiently in mosquito cells, and this was explained by the
171 fact that R243A/K245A had reverted to WT in mosquito cells allowing efficient replication.
172 To test this assumption, total RNA from U4.4 and C6/36 cells at 72 h.p.t was extracted,
173 amplified by RT-PCR and sequenced. Surprisingly, none of the AUD mutants had
174 reverted to WT, and all three mutants retained the same sequence as the input RNA (Fig
175 2C). The results demonstrated that the ability of these three AUD mutants to replicate in
176 mosquito cells was not due to reversion.

177 To confirm that the phenotype of the three AUD mutants was not specific to C2C12 cells
178 we further investigated this in other mammalian cells. These included RD (a human
179 rhabdomyosarcoma cell line), two human hepatoma cell lines, Huh7 and Huh7.5 and
180 BHK-21 hamster kidney fibroblast cells. Huh7.5 are derived from Huh7, and due to a
181 mutation in one allele of the retinoic acid-inducible gene I (RIG-I) [39], a cytosolic pattern
182 recognition receptor responsible for the type 1 interferon (IFN) response, Huh7.5 cells are
183 defective in innate immunity. Reassuringly, all three AUD mutants showed replication
184 defects compared to WT in all these cell lines (Fig 2D), although the magnitude of the
185 defective phenotypes varied between different cell lines. In particular the defective
186 phenotypes were less apparent in BHK-21 cells, this is consistent with our observations
187 of other mutants in nsP3 [40]. We conclude that the three residues W220, D249 and

188 Y324 within the CHIKV nsP3 AUD play a role in genome replication in mammalian cells
189 but not in mosquito cells.

190 The AUD mutants exhibit a temperature dependent phenotype

191 We reasoned that a simple explanation for the different phenotypes in mammalian and
192 mosquito cells might be the temperature difference, as mammalian cells are cultured at
193 37°C whereas mosquito cells are cultured at 28°C [41]. To test this, the replication of WT
194 and mutant SGR-D-Luc were analysed in C2C12 cells incubated at 37°C or 28°C.
195 Surprisingly, the replication of the three mutants was indistinguishable from WT at 28°C
196 (Fig 3A), in addition we noted that for WT SGR-D-Luc, replication rates were similar at
197 both temperatures up to 12 h.p.t. However, at 28°C replication continued to increase
198 (approximately 100-fold) from 12 to 24 h.p.t, whereas at 37°C it peaked at 12 h.p.t. It
199 should be noted that the optimal temperature for FF-Luc activity is between 22-28°C [42],
200 so to confirm that this observation reflected a bona fide effect on genome replication,
201 rather than increased activity of the FF-Luc reporter at the lower temperature, translation
202 of CHIKV SGR at the two temperatures was quantified by western blotting for nsP1
203 expression (Fig 3B). Reassuringly, none of the mutants exhibited detectable nsP1 at
204 37°C whereas a low level of nsP1 was detectable for the WT at this temperature. In
205 contrast WT and all mutants exhibited high levels of nsP1 at 28°C, consistent with the
206 elevated levels of replication and translation at this temperature. In addition, we saw the
207 same phenotype when levels of R-Luc were measured (S2 Fig).

208 We also observed the same results in two other mammalian cell lines, Huh7 and Vero
209 (Fig 3C, D). Vero are African Green Monkey kidney epithelial cells and are IFN-deficient

210 thus unable to mount an IFN response following virus infection (although they possess
211 IFN receptors and can response to exogenous IFN). Our data suggest that the enhanced
212 replication at 28°C is not due to the previously documented reduced efficiency of the IFN
213 response at sub-physiological temperatures [43].

214 We conclude that the three AUD mutants (W220A, D249A and Y324A) are temperature
215 sensitive, exhibiting no defective phenotype in mammalian cells at a sub-physiological
216 temperature. However, we also note the novel observation that replication of WT CHIKV
217 SGR is significantly enhanced at sub-physiological temperature.

218 Enhanced replication at sub-physiological temperature is not 219 dependent on the nature of the nsP3-fused reporter protein and is 220 alphavirus specific.

221 As the SGR-D-Luc construct contains two reporters, we considered it prudent to confirm
222 that the phenotype we observed was not influenced by these reporters. To test this, two
223 alternative CHIKV SGRs were utilised, namely SGR-nsP3-mCh-FF-Luc (in which the R-
224 Luc reporter was replaced with mCherry) and SGR-FF-Luc (lacking R-Luc and thus
225 expressing WT unfused nsP3) (Fig 4A). These three SGRs were assayed in three cell
226 types, C2C12, Huh7 and Vero cells at the two temperatures (28°C or 37°C). All three
227 showed enhanced levels of replication at 28°C compared to 37°C (Fig 4B-D). As
228 described previously (Fig 3A), this effect was most apparent between 12-24 h.p.t.

229 We reasoned that the enhancement of genome replication at sub-physiological
230 temperature might be a common feature in other arboviruses that would share a mode of
231 transmission from mosquitoes to humans via a peripheral bite. We therefore tested

232 replication of mini-genome constructs derived from Bunyamwera virus (BUNV), the type
233 species of the bunyaviridae (negative-sense, single-stranded RNA viruses) [44] and an
234 SGR derived from Zika virus, a positive-sense, single-stranded RNA virus in the
235 Flaviviridae family [45]. As shown in Fig 4E and F, both the BUNV mini-genome [46] and
236 the Zika virus SGR [47] showed similar levels of genome replication at physiological and
237 sub-physiological temperatures (Fig 4F), indicating that this phenotype is specific to
238 alphaviruses.

239 Overall, data from three CHIKV SGRs at different temperatures confirmed that enhanced
240 genome replication at sub-physiological temperature is not dependent on the nature of
241 the nsP3-fused reporter protein and is specific to alphavirus.

242 Temperature sensitive AUD mutants retain the phenotype in the 243 context of infectious CHIKV and O'Nyong Nyong virus (ONNV).

244 As we had previously identified a novel function of the CHIKV AUD in promoting virus
245 assembly, we wished to determine whether the phenotypes we had observed in the
246 context of CHIKV SGR were also seen in infectious virus. The three AUD mutations
247 (W220A, D249A and Y324A) were therefore generated in the backbone of the ICRES-
248 CHIKV infectious clone [36]. In vitro transcribed RNA for each construct was transfected
249 into C2C12 cells and released virus were harvested at 48 h post infection (h.p.i) and
250 titrated by plaque assay on BHK-21 cells. As shown in Fig 5A, the three mutants
251 produced significantly less infectious virus than WT at 37°C (approx. 10^4 reduction in titre).
252 At 28°C, unlike the SGR data where the mutants were indistinguishable from WT, the
253 mutants exhibited significantly reduced titres although this phenotype was less

254 pronounced than at 37°C (between 5-50 fold reduction). Sequence analysis of ICRES-
255 CHIKV AUD mutants at 28°C or 37°C indicated that no reversion had occurred at either
256 temperature (data not shown). However, unlike the marked differences in genome
257 replication observed using SGRs, there was only a modest increase (2-fold) in virus
258 production at 28°C compared to at 37°C. This suggested that the higher level of genome
259 replication at 28°C did not lead to a concomitant increase in assembly and release of
260 infectious virus.

261 We also extended this analysis to a closely related virus, ONNV, which can be
262 manipulated at BSL2. We exploited an infectious clone of ONNV in which the fluorescent
263 reporter ZsGreen is expressed on a sgRNA driven from a second copy of the sub-
264 genomic promoter (ONNV-2SG-ZsGreen) (Fig 5B) (kind gift from Prof. Andres Merits,
265 University of Tartu). This enables rapid assessment of genome replication by
266 quantification of ZsGreen fluorescence per cell, as well as simultaneous measurement of
267 infectious virus production by quantification of ZsGreen positive cells. It should be noted
268 that although expression of ZsGreen is dependent on genome replication as production
269 of the sgRNA is templated from the negative strand, the levels of ZsGreen expression will
270 be representative of both replication and translation of the sgRNA. We also observed
271 that the three AUD mutants exhibited a temperature dependent replication phenotype in
272 the context of ONNV (Fig 5C). At 28°C the level of ZsGreen expression per cell was
273 indistinguishable between WT and the three AUD mutants, whereas at 37°C the mutants
274 showed a significant reduction in ZsGreen expression per cell. Interestingly, in contrast
275 to the CHIKV results, sequence analysis revealed that at 37°C, W220A and D249A had
276 reverted to WT and Y324A exhibited two compensatory pseudorevertant mutations (nsP2

277 R768Q and nsP3 C173Y) (data not shown), however, no reversion was observed for the
278 AUD mutants at 28°C. Interestingly, we noticed a significant difference in virus production
279 with plaque assays conducted at different temperatures. Due to the fact that the AUD
280 mutants had reverted at 37°C, there were no significant differences in virus production at
281 37°C when the virus was titrated at either 37°C or 28°C (Fig 5D). In contrast, when
282 viruses were produced at 28°C and titrated at 28°C, the AUD mutants exhibited virus
283 titres indistinguishable from WT, whereas when titrated at 37°C they showed significant
284 reduction in virus titres compared to WT. These data confirm that mutant viruses
285 produced at 28°C retained the growth defects at 37°C.

286 Temperature shift assay reveals that early events in SGR-D-Luc 287 replication are not enhanced at sub-physiological temperature

288 Previous studies have investigated temperature-sensitive mutants of alphaviruses by use
289 of a temperature shift assay [48-50]. To further explore the role of temperature in
290 controlling CHIKV genome replication, a temperature shift assay using WT SGR-D-Luc
291 was conducted in C2C12 cells. WT SGR-D-Luc RNA was transfected into C2C12 cells
292 and incubated either at 37°C or 28°C for 12 h, with and without a subsequent temperature
293 shift from 12-24 h.p.t (28°C to 37°C (designated S*) or 37°C to 28°C (designated S#))
294 (Fig 6A). As seen previously (Fig 3A), replication of WT SGR-D-Luc (as assessed by
295 FLuc levels) up to 12 h.p.t proceeded at broadly similar rates at both temperatures (Fig
296 6B), and between 12-24 h.p.t replication increased ~100-fold at 28°C but did not increase
297 at 37°C. However, if the temperature was shifted from 28°C to 37°C at 12 h.p.t (S*), the
298 replication increased only ~20-fold between 12-24 h.p.t (Fig. 6B, left graph). The opposite
299 effect was seen when transfected cells were first incubated at 37°C: replication reduced

300 slightly between 12-24 h.p.t at 37°C, however, when temperature was shifted from 37°C
301 to 28°C at 12 h.p.t, replication increased 5-fold between 12-24 h.p.t (Fig. 6B, right graph).

302 Importantly, both cell growth assessed by quantification of viable cells (Fig 6C), and
303 metabolic activity assessed by MTT assay (Fig 6D) were higher at 37°C compared to
304 28°C. Temperature shifts elicited the expected changes in both cell number and
305 metabolic activity. As expected therefore, these data confirmed that the enhanced
306 replication observed at sub-physiological temperature cannot be explained by increased
307 cell growth and metabolic activity. In fact we observed the opposite, virus genome
308 replication was elevated when cell growth and metabolic activity was dampened at the
309 lower temperature. These data were also confirmed by Western blotting for nsP1 (Fig
310 6E), demonstrating that translation of the 5' ORF was also enhanced at the sub-
311 physiological temperature. At this stage we also asked whether the replication level was
312 correlated with the level of phosphorylated eIF2α (P-eIF2α), given that this is a critical
313 factor in restricting translation during cell stress. However, there appeared to be little
314 correlation between replication and levels of P-eIF2α (Fig 6C), with the exception that
315 when the temperature was shifted from 37°C to 28°C at 12 h.p.t. (S#), P-eIF2α levels
316 reduced, coincident with an increase in replication (Fig 6B, right hand graph).

317 Inhibition of eIF2α phosphorylation failed to recover replication defects
318 of the AUD mutants at 37°C

319 To follow up on the possible role of eIF2α phosphorylation in the enhancement of genome
320 replication at sub-physiological temperature, we exploited the well-characterised
321 compound ISRIB which reverses the effects of eIF2α phosphorylation [51, 52]. As shown

322 in Fig 7A, replication of both WT and W220A SGR-D-Luc was enhanced 5-fold by 200
323 nM ISRIB at 28°C, suggesting that eIF2α phosphorylation may make a minor contribution
324 to the higher level of replication at this sub-physiological temperature. However, at 37°C
325 ISRIB treatment resulted in a 2-fold increase in replication for WT SGR-D-Luc but had no
326 effect on W220A SGR-D-Luc (Fig 7A). ISRB was titrated over a 100-fold concentration
327 (200 nM – 20 μM) and the stimulatory effect was apparent at the lowest concentration
328 with no cytopathic effect (S3 Fig). Similar results were observed in the context of ONNV
329 infection (Fig 7B): ISRIB enhanced replication of both WT and W220A at 28°C, but at
330 37°C only WT was enhanced. These data indicated that pharmacological inhibition of the
331 effects of eIF2α phosphorylation by ISRIB was able to stimulate alphavirus genome
332 replication at 28°C, however, ISRIB treatment of WT at 37°C only modestly enhanced
333 replication and did not recapitulate the differences observed at the sub-physiological
334 temperature (eg Fig 3). In addition, ISRIB treatment did not restore the replication ability
335 of the W220A mutant at the non-permissive temperature.

336 Alterations in stress granule formation in response to ONNV infection 337 at physiological and sub-physiological temperatures

338 In a further attempt to shed light on the reasons why alphavirus genome replication was
339 enhanced in mammalian cells at sub-physiological temperature we turned our attention
340 to stress granules (SG). These are large cytoplasmic foci that are nucleated by the
341 aggregation of 48S mRNPs, which accumulate following stress-induced translation arrest
342 [53]. SG contain aggregates of stalled, translationally silent mRNAs, initiation factors,
343 small ribosomal subunits, and mRNA binding proteins [54]. Although SG have been
344 shown to be antiviral, paradoxically alphavirus infection has been reported to induce SG

345 and nsP3 has been shown to interact with SG components, in particular G3BP1/2, to
346 modulate their composition [32, 55]. SG formation can be induced by treatment with
347 sodium arsenite ($NaAsO_2$) which results in oxidative stress, and they can be
348 disassembled by CHX treatment. We considered that SG formation might be relevant in
349 this investigation as it had been previously shown that $NaAsO_2$ was only able to induce
350 SG at 37°C but not 28°C [29]. We confirmed that this was also the case in our hands (Fig
351 8A, B), as no G3BP1-positive SG were observed following $NaAsO_2$ treatment at 28°C.

352 We proceeded to analyse G3BP1-positive SG in cells infected with ONNV-ZsGreen at
353 both temperatures. Both the number and size of SG were determined in 10 cells and
354 compared to those induced by $NaAsO_2$. ZsGreen positivity enabled us to identify infected
355 cells. In contrast to the inability of $NaAsO_2$ to induce SG at 28°C, ONNV infection was
356 able to induce SG at both temperatures. Interestingly, the G3BP1-positive SG induced
357 by ONNV infection differed significantly in both size and number at the two temperatures
358 (Fig 9A, B). We observed that at 28°C the average cross-sectional area of SG was
359 significantly smaller than at 37°C (mean 0.5 μm^2 compared to ~1.6 μm^2), although both
360 of these were also significantly smaller than those induced by $NaAsO_2$ at 37°C (mean
361 ~4.5 μm^2). In addition, CHX treatment reduced the size of ONNV-induced SG from a
362 mean of 1.6 μm^2 to ~0.8 μm^2 at 37°C, whereas at 28°C CHX treatment had no effect on
363 SG size. In contrast, ONNV infection at 28°C resulted in a larger number of SG compared
364 to at 37°C, and infection at both temperatures resulted in more SG than after $NaAsO_2$
365 treatment (Fig. 9B).

366 We also analysed the presence of dsRNA in ONNV-infected cells as a direct indicator of
367 genome replication using the dsRNA-specific antibody, J2. Consistent with our previous

368 results using CHIKV SGR (Fig 3), we saw a higher level of dsRNA in cells infected at
369 28°C compared to 37°C (Fig. 9C), indicating elevated genome replication at the sub-
370 physiological temperature. However, quantification of ZsGreen in individual cells
371 revealed lower levels at 28°C compared to at 37°C, further evidence that the enhanced
372 levels of genome replication seen at the sub-physiological temperature did not directly
373 correlate with increased translation from the sgRNA.

374 The difference in the sizes of SG induced by either $NaAsO_2$ or ONNV at the two
375 temperatures led us to ask whether there were any gross differences in their composition.
376 Cells treated with $NaAsO_2$ or infected with ONNV were therefore analysed by indirect
377 immunofluorescence for two other well-characterised SG components: the mRNA binding
378 protein T-cell-restricted antigen 1 (TIA-1) and the translation initiation factor eIF4G [56].
379 As shown in Fig 10A/B, SG induced by $NaAsO_2$ at 37°C contained both TIA-1 and eIF4G,
380 and consistent with the lack of G3BP1-positive SG at 28°C, neither TIA-1 or eIF4G
381 accumulated into SG at 28°C. In contrast, following ONNV infection TIA-1 positive SG
382 were observed at both temperatures but eIF4G did not accumulate into SG at either
383 temperature. These data are consistent with the previous observations [33] that SG
384 induced by alphavirus infection are compositionally distinct from those induced by other
385 cellular stresses, however they do not shed any light on the different seen in ONNV-
386 induced SG at the two temperatures.

387

388 # Discussion

389 This study started with the intention of building on our previous work which identified a
390 role for two residues (P247 and V248) in the function of the CHIKV AUD [15]. Alanine
391 substitution of these residues (termed the PV mutant) disrupted the binding of the AUD
392 to the sub-genomic promoter, reducing levels of structural proteins with concomitant
393 effects on virus assembly. In this study we generated a series of mutations in surface
394 exposed and conserved residues proximal to P247 and V248 to further investigate the
395 phenotype. Surprisingly, most of these mutations had no effect on genome replication,
396 although we cannot rule out an effect on virus assembly as this was not evaluated in this
397 study. However, our experiments did demonstrate a role in genome replication for three
398 residues W220, D249 and Y324, interestingly these residues are distal from each other
399 (Fig 1B). Indeed, Y324A was chosen as a control, being defined as the last residue in
400 the AUD [34]. The phenotypes of the 3 mutants were observed in all mammalian cells
401 tested although the magnitude of the defects varied somewhat. Intriguingly, in BHK-21
402 cells the mutants appeared to be better tolerated, as seen previously for both PV [15] and
403 mutations in the nsP3 macrodomain [40]. Our study took a surprising turn when we
404 observed that the 3 mutants exhibited no defective phenotype in mosquito cells and also
405 when assayed in mammalian cells at sub-physiological temperatures, defining these as
406 temperature-sensitive (ts) mutants. This analysis also revealed that the wildtype CHIKV
407 replicated more efficiently at sub-physiological temperatures in mammalian cells and we
408 focused our attentions on this intriguing observation.

409 As 28°C is a very low temperature for the growth of mammalian cells, we also tested the
410 phenotype of W220A at an intermediate temperature, 32°C, likely to be better tolerated

411 by cells in culture. Reassuringly, W220A replicated as well as WT at this temperature
412 and WT was itself more efficient than at 37°C (S4 Fig). It should be noted that ts mutations
413 in alphavirus nsP3 have been previously identified, for example in Sindbis virus F312S
414 and A268V both resulted in a defect in negative-strand RNA synthesis at the non-
415 permissive temperature (40°C) [57]. In addition, a macro-domain mutant A68G had a
416 partial phenotype. These data point to a critical role of nsP3, and the AUD in particular,
417 in genome replication. Further biochemical analysis of these ts mutants in nsP3 may
418 shed light on the specific role of nsP3.

419 In considering why alphavirus genome replication in mammalian cells might be enhanced
420 at sub-physiological temperatures, we reasoned that the first cells infected via a mosquito
421 bite would be in the periphery and thus not at 37°C. It would be reasonable to expect that
422 other arboviruses would also exhibit the same differential, however, that was not the case
423 as both BUNV and ZIKV replicated to similar levels at 28°C and 37°C. This suggested
424 that this phenotype would be driven by alphavirus specific processes, and we noted that
425 both the nsP3 macrodomain and the AUD do not have functional homologues in either
426 bunyaviruses or flaviviruses. Analysis of the timescale of genome replication at different
427 temperatures also revealed that the phenotype was most apparent after 12 h.p.t. In most
428 cases, replication rates up to 12 h.p.t. did not differ between the two temperatures (eg
429 see Fig 3A), however between 12-24 h.p.t. replication continued to increase at 28°C, but
430 plateaued at 37°C. One interpretation for this observation is that this reflects an aspect
431 of the cellular response to virus genome replication that is perhaps ablated or blunted at
432 the sub-physiological temperature. An obvious candidate would be the type 1 IFN
433 response, which has indeed been shown to be reduced at lower temperatures promoting

434 CHIKV arthritis in a mouse model [58]. However, our data suggest that this is not the
435 explanation for our findings as we observed the same phenotype in Vero and Huh7.5
436 cells, both of which are defective in aspects of the IFN response.

437 An alternative possibility was that the host cell translational shutoff mediated by the
438 phosphorylation of eIF2α was impaired at sub-physiological temperatures. However, we
439 were unable to determine any specific correlation between eIF2α phosphorylation and
440 genome replication (eg see Fig 6C). In addition, treatment with ISRIB, a small molecule
441 that reverses the effects of eIF2α phosphorylation [52], failed to recapitulate the effect of
442 the lower temperature on replication of wildtype CHIKV or ONNV at 37°C, and did not
443 permit the replication of W220A at 37°C. We therefore turned our attention to stress
444 granules (SG), cytoplasmic protein-mRNA aggregates formed in response to stress and
445 believed to play an antiviral role. The link between alphavirus infection and SG formation
446 is confusing, as alphaviruses induce formation of SG that differ in composition from
447 canonical SG induced by other stressors, yet two key components of SG, GTPase-
448 activating protein (SH3 domain)-binding proteins 1 and 2 (G3BP1/2), are critical for
449 alphavirus genome replication [27].

450 As seen previously [29], treatment with $NaAsO_2$ (which induces oxidative stress) did not
451 result in SG formation at 28°C, suggesting that there was a defect in this process at the
452 sub-physiological temperature. However, alphavirus (ONNV) infection did induce SG
453 formation at both temperatures – the composition of these SG was comparable (Fig 10)
454 but both their size and quantity were different (Fig 9 B/C). Specifically, at 28°C SG were
455 smaller, more numerous and were not disassembled by CHX treatment. To attempt to
456 understand why the formation of smaller and more numerous SG might promote genome

457 replication, we calculated the mean surface area and volume of SG per cell. To do this
458 we assumed that SG are spherical and used the following parameters: at 28°C the mean
459 cross-sectional area of SG was 0.5 μm^2 (radius = 0.4 μm) and the mean number per cell
460 were 65, at 37°C the mean cross-sectional area of SG was 1.6 μm^2 (radius = 0.7 μm) and
461 the mean number per cell were 29 (Fig 9B). Using these parameters at 28°C the mean
462 surface area of SG was 123 μm^2 per cell and the mean volume was 1.6 μm^3 per cell. At
463 37°C the mean surface area of SG was 178 μm^2 per cell and the mean volume was 41.6
464 μm^3 per cell. Therefore, the volume of SG at 37°C was 26-fold greater than at 28°C. One
465 possible interpretation of this is that the smaller volume of SG at the sub-physiological
466 temperature limited the sequestration of proteins such as G3BP1/2 that are required for
467 genome replication, allowing that process to continue. Why the process of alphavirus-
468 driven SG formation should differ at different temperatures remains to be determined,
469 however, importantly the ADP-ribosylhydrolase activity of the nsP3 macro-domain has
470 recently been shown to play a key role in SG formation, disassembly and composition
471 [33]. It is possible that the enzymatic activity and/or substrate specificity of the
472 macrodomain could be modulated by temperature. Although the AUD *per se* has not
473 been directly shown to play a role in SG formation, it is flanked by the macro-domain and
474 HVD, both of which now have been implicated in SG formation. It is thus possible that all
475 three domains of nsP3 coordinate to control SG formation and enable genome replication.

476 In conclusion, our data have revealed a hitherto unrecognized enhancement of alphavirus
477 genome replication in mammalian cells at sub-physiological temperature that may play a
478 role in the early stages of transmission of virus to the mammalian host via a mosquito bite.
479 Our observations point to a critical role of the AUD in this difference, and our ongoing

480 work seeks to understand the effects of temperature on the nsp3 interactions with host
481 cell proteins using a proteomic approach.

482 Material and methods

483 Sequence alignment

484 AUD amino acid sequences in a variety of alphaviruses (Sindbis, Semiliki, Ross Rover,
485 Venezuelan, Eastern and Western Equine Encephalitis, ONNV and CHIKV) were
486 obtained from NCBI and aligned by Clustal Omega. The conserved AUD residues were
487 identified by Pymol and their locations were predicated from the Sindbis nsP2/3 protein
488 structure (PDB ID code 4GUA) [15].

489 Cell culture

490 Mammalian cells RD, Huh7, Huh7.5, Vero and BHK-21 cells were in DMEM supplied with
491 10% Fetal Calf Serum (FCS), 0.5 mM non-essential amino acids and penicillin-
492 streptomycin (100 units/mL). C2C12 cells were supplied with the same components apart
493 from 20% FCS. All mammalian cells were maintained at 37°C or 28°C with 5% CO_2. RD
494 cells were obtained from Nicola Stonehouse (University of Leeds), Huh7 cells were
495 obtained from John McLauchlan (Centre for Virus Research, Glasgow), Huh7.5 cells were
496 obtained from Charles Rice (Rockefeller University, New York), BHK-21 cells were
497 obtained from John Barr (University of Leeds), C2C12 cells were obtained from Michelle
498 Peckham (University of Leeds). U4.4 and C6/36 cell lines (*Ae. albopictus*) were obtained
499 from Susan Jacobs (The Pirbright Institute) and were cultured in Leibovitz's L-15 media

500 containing 10% FCS, 10% tryptose phosphate broth and penicillin-streptomycin (100
501 units/mL), at 28°C without CO_2.

502 Plasmid constructs

503 SGR-D-Luc was used as a template for site-directed mutagenesis using specific primers
504 to generate each of the AUD mutations. The AUD mutated fragments were excised and
505 ligated into the SGR-D-Luc backbone. AUD mutated fragments were also ligated into the
506 infectious ICRES-CHIKV clone [36]. For construction of the ONNV AUD mutants, a
507 fragment including the AUD coding sequence was excised from the ONNV-2SG-ZsGreen
508 (donated by Prof. Andres Merits, University of Tartu), and ligated into pcDNA3.1 to
509 generate pcDNA3.1-ONNV-AUD. This was used as a template for site-directed
510 mutagenesis using specific primers to generate ONNV AUD mutations. The ONNV AUD
511 mutated fragments were excised from pcDNA3.1-ONNV-AUD and ligated into the ONNV-
512 2SG-ZsGreen backbone. SGR-nsP3-mCh-FF-Luc was generated by SpeI digestion of
513 the FF-Luc fragment from SGR-D-Luc and insertion of the mCherry coding sequence.
514 SGR-FF-Luc was constructed by SpeI digestion of the FF-Luc fragment from SGR-D-Luc
515 and self-ligation.

516 Transfection and Dual-luciferase Assay

517 Capped RNAs of WT and mutant SGR-D-Luc, ICRES-CHIKV, ONNV-2SG-ZsGreen, or
518 WT SGR-nsP3-mCh-FF-Luc, WT SGR-FF-Luc were synthesized and purified using the
519 mMACHINE™ SP6 Transcription Kit (Thermo Fisher Scientific). In brief, 250 ng of each
520 of the RNAs was transfected into 5 x 10^4 cells using Lipofectamine 2000 (Life
521 Technologies) according to the manufacturer's instructions. Cells were harvested at 4, 12,

522 24 or 48 h.p.t. and both FF-Luc and R-Luc activities were measured using the Dual-
523 luciferase Kit (Promega) according to the manufacturer's instruction. The experiments
524 were repeated three times independently.

525 Sequence analysis

526 Total RNA from transfected or infected cells was extracted by Trizol, followed by reverse
527 transcription to generate cDNA using the SuperScript IV Reverse Transcriptase
528 (Invitrogen) according to the manufacturer's instruction. The expected DNA fragments of
529 CHIKV or ONNV genome were amplified by PCR using specific primers (Primer
530 sequences available upon request). Then all PCR products were sequenced.

531 Temperature shift assay

532 C2C12 cells were transfected with WT SGR-D-Luc RNA and incubated at 28°C or 37°C,
533 with and without a temperature shift from 12-24 h.p.t (from 28°C to 37°C (designated S*)
534 or 37°C to 28°C (designated S#)). Cells were harvested at 4, 12 and 24 h.p.t. All the cells
535 were then lysed and measured using a dual luciferase kit (Promega), nsP1 expression
536 were also detected by western blotting. Along with the temperature shift assay, cell growth
537 number at 37°C or 28°C were counted by trypsin treatment and dilution into 1 ml of DMEM
538 and cell metabolic activity at two temperatures was assessed by MTT assay.

539 MTT assay

540 C2C12 cells were seeded into 96 well plates. The next day, cells were mock transfected
541 and incubated at 37°C or 28°C. At 4, 12 or 24 h.p.t, cell media were removed and replaced
542 with 150 μl phenol-red free DMEM media and 30 μl 6 mM MTT. Cells were incubated at

543 37°C for 2 h before media were removed and replaced with 100 µl DMSO. Then cells
544 were covered with foil and agitated until all MTT granules had dissolved, prior to reading
545 absorbance at 570 nm.

546 Plaque assay

547 As described above, cell supernatants were harvested 48 h.p.i and stored at -80°C.
548 Supernatants were thawed, serially diluted and applied to monolayers of BHK-21 cells for
549 1 h at 37°C. The inocula were aspirated and cells were overlaid with 0.8% methylcellulose
550 for 72 h at 37°C, 96 h at 28°C for ONNV infection, and 48 h at 37°C for ICRES-CHIKV.
551 Plaques were either visualized by EVOS microscopy (ONNV) or staining with 0.05%
552 crystal violet for 30 min (CHIKV).

553 ISRIB assay

554 C2C12 cells were transfected with WT SGR-D-Luc or mock transfected, and 200 nM
555 ISRIB was added to cells at 2 h.p.t. Cells were then harvested at 4, 12, 24 h.p.t. and dual
556 luciferase activities were measured. For ONNV infection, C2C12 cells were infected with
557 WT and W220A ONNV at an MOI of 0.1 for 1 h at 37°C, washed with PBS 3 times and
558 replaced with complete media containing 200 nM ISRIB prior to incubation at 28°C or
559 37°C. Levels of nsP1, eIF2α, P-eIF2α were detected by western blotting.

560 Western blotting

561 Cells were lysed in 1X passive lysis buffer (PLB) or 1X Glasgow Lysis Buffer (GLB)
562 supplemented with protease inhibitors and phosphatase inhibitors (Roche Diagnostics,
563 specific for detection of P-eIF2α), protein samples were quantified by BCA assay (Pierce)

564 according to manufacturer's instruction. 10 or 20 µg of each protein samples was heat
565 denatured at 95°C for 5 min and separated by SDS-PAGE, proteins were then transferred
566 to polyvinylidene fluoride (PVDF) membrane and blocked with 50% (v/v) Odyssey
567 blocking buffer (Li-Cor) diluted in 1X Tris-buffered saline tween-20 (TBST) (50 mM Tris,
568 150 mM NaCl, 0.1% Tween-20, pH 7.4). The membrane was then incubated with primary
569 antibodies (1:1000 dilution) at 4°C overnight and the next day incubated with fluorescently
570 labelled anti-mouse (700 nm) and anti-rabbit (800 nm) secondary antibodies for 1 h at
571 room temperature (RT). Membranes were then imaged on a Li-Cor Odyssey Sa Imager
572 (Li-cor).

573 **Immunofluorescence assay**

574 RD cells were seeded into 12 well plates with coverslips. The next day, cells were infected
575 with WT ONNV at an MOI of 5 by incubating inoculum at 37°C for 1 h and then replaced
576 with complete media. Mock infected cells were treated with 0.5 mM $NaAsO_2$ for 1 h at 7
577 h.p.i, then cells were either fixed by 4% formaldehyde or treated with 100 µg/ml CHX for
578 45 min and then fixed by 4% formaldehyde. Cells infected with WT ONNV were also
579 treated with 100 µg/ml CHX for 45 min at 8 h.p.i and then fixed with 4% formaldehyde.
580 Cells were washed with PBS, permeabilized with ice-cold methanol at -20 °C for 10 min
581 and blocked with 2% BSA for 1 h. The cells were incubated with primary antibody to
582 G3BP1 (Abcam) (1:200), eIF4G (Thermo) (1:100 dilution) or TIA (Thermo) (1:100 dilution),
583 or a combination of G3BP (Proteintech) (1:100) and P-eIF2α (Thermo Fisher) (1:100) at
584 4°C overnight. The next day, cells were washed with DEPC-PBS and incubated with J2
585 dsRNA antibody (Scicons) (1:100 dilution) at RT for 1 h. All cells were stained with Alexa
586 Fluor-594 chicken anti-rabbit and Alexa Fluor-647 goat anti-mouse secondary antibodies

587 (1:500 dilution) at RT for 1 h. Cells were mounted onto glass slides with Prolong Gold
588 antifade reagent (Invitrogen) containing 4',6'-diamidino-2-phenylindole dihydrochloride
589 (DAPI) and sealed with nail varnish. Confocal microscopy images were acquired using a
590 Zeiss LSM880 upright microscope. Post-acquisition analysis of images was performed
591 using Zen software (Zen version 2018 black edition 2.3, Zeiss), or Fiji imageJ (v1.49)
592 software.

593 **Statistical analysis**

594 Statistical analysis was performed using the unpaired Student's t tests (two-tailed). Data
595 in bar graphs represent statistically significant differences and displayed as the means ±
596 S.E. of three experimental replicates (n = 3).

597 **Acknowledgments**

598 We thank Prof. Andres Merits (Institute of Technology, University of Tartu, Estonia) for
599 the CHIKV SGRs, ICRES constructs, ONNV-2SG-ZsGreen construct and antibody to
600 nsP1. We thank Dr. Andrew Tuplin for the Zika virus replicon and Dr John Barr for the
601 BUNV mini-genome construct. We thank Drs. Niluka Goonawardane and Ruth Hughes
602 for help in Fiji imageJ analysis. We also thank Dr Sreenivasan Ponnambalam for access
603 to the EVOS microscope.

604 **Funding**

605 This work was supported by a Wellcome Investigator Award to MH (grant number
606 096670). JG was supported by a University of Leeds/China Scholarship Council PhD

607 studentship. The funders had no role in study design, data collection and analysis,
608 decision to publish, or preparation of the manuscript.

609 # References

610 [1] R. Chen, S. Mukhopadhyay, A. Merits, B. Bolling, F. Nasar, L.L. Coffey, A. Powers,
611 S.C. Weaver, C. Ictv Report, ICTV Virus Taxonomy Profile: Togaviridae, J Gen Virol 99(6)
612 (2018) 761-762.
613 [2] O. Schwartz, M.L. Albert, Biology and pathogenesis of chikungunya virus, Nat Rev
614 Microbiol 8(7) (2010) 491-500.
615 [3] M.C. Robinson, An epidemic of virus disease in Southern Province, Tanganyika
616 Territory, in 1952-53. I. Clinical features, Trans R Soc Trop Med Hyg 49(1) (1955) 28-32.
617 [4] W.H. Lumsden, An epidemic of virus disease in Southern Province, Tanganyika
618 Territory, in 1952-53. II. General description and epidemiology, Trans R Soc Trop Med
619 Hyg 49(1) (1955) 33-57.
620 [5] I. Schuffenecker, I. Iteman, A. Michault, S. Murri, L. Frangeul, M.C. Vaney, R. Lavenir,
621 N. Pardigon, J.M. Reynes, F. Pettinelli, L. Biscornet, L. Diancourt, S. Michel, S. Duquerroy,
622 G. Guigon, M.P. Frenkiel, A.C. Brehin, N. Cubito, P. Despres, F. Kunst, F.A. Rey, H. Zeller,
623 S. Brisse, Genome microevolution of chikungunya viruses causing the Indian Ocean
624 outbreak, PLoS Med 3(7) (2006) e263.
625 [6] K. Sergon, C. Njuguna, R. Kalani, V. Ofula, C. Onyango, L.S. Konongoi, S. Bedno, H.
626 Burke, A.M. Dumilla, J. Konde, M.K. Njenga, R. Sang, R.F. Breiman, Seroprevalence of
627 Chikungunya virus (CHIKV) infection on Lamu Island, Kenya, October 2004, Am J Trop
628 Med Hyg 78(2) (2008) 333-7.

629 [7] A.J. Tatem, S.I. Hay, D.J. Rogers, Global traffic and disease vector dispersal, Proc
630 Natl Acad Sci U S A 103(16) (2006) 6242-7.
631 [8] O.J. Brady, M.A. Johansson, C.A. Guerra, S. Bhatt, N. Golding, D.M. Pigott, H. Delatte,
632 M.G. Grech, P.T. Leisnham, R. Maciel-de-Freitas, L.M. Styer, D.L. Smith, T.W. Scott, P.W.
633 Gething, S.I. Hay, Modelling adult Aedes aegypti and Aedes albopictus survival at
634 different temperatures in laboratory and field settings, Parasit Vectors 6 (2013) 351.
635 [9] E.A. Mordecai, J.M. Cohen, M.V. Evans, P. Gudapati, L.R. Johnson, C.A. Lippi, K.
636 Miazgowicz, C.C. Murdock, J.R. Rohr, S.J. Ryan, V. Savage, M.S. Shocket, A. Stewart
637 Ibarra, M.B. Thomas, D.P. Weikel, Detecting the impact of temperature on transmission
638 of Zika, dengue, and chikungunya using mechanistic models, PLoS Negl Trop Dis 11(4)
639 (2017) e0005568.
640 [10] J.C. Rupp, K.J. Sokoloski, N.N. Gebhart, R.W. Hardy, Alphavirus RNA synthesis and
641 non-structural protein functions, J Gen Virol 96(9) (2015) 2483-2500.
642 [11] H. Malet, B. Coutard, S. Jamal, H. Dutartre, N. Papageorgiou, M. Neuvonen, T. Ahola,
643 N. Forrester, E.A. Gould, D. Lafitte, F. Ferron, J. Lescar, A.E. Gorbalenya, X. de
644 Lamballerie, B. Canard, The crystal structures of Chikungunya and Venezuelan equine
645 encephalitis virus nsP3 macro domains define a conserved adenosine binding pocket, J
646 Virol 83(13) (2009) 6534-45.
647 [12] L. Eckei, S. Krieg, M. Butepage, A. Lehmann, A. Gross, B. Lippok, A.R. Grimm, B.M.
648 Kummerer, G. Rossetti, B. Luscher, P. Verheugd, The conserved macrodomains of the
649 non-structural proteins of Chikungunya virus and other pathogenic positive strand RNA
650 viruses function as mono-ADP-ribosylhydrolases, Sci Rep 7 (2017) 41746.

651 [13] R.L. McPherson, R. Abraham, E. Sreekumar, S.E. Ong, S.J. Cheng, V.K. Baxter, H.A.
652 Kistemaker, D.V. Filippov, D.E. Griffin, A.K. Leung, ADP-ribosylhydrolase activity of
653 Chikungunya virus macrodomain is critical for virus replication and virulence, Proc Natl
654 Acad Sci U S A 114(7) (2017) 1666-1671.
655 [14] N.J. Foy, M. Akhrymuk, A.V. Shustov, E.I. Frolova, I. Frolov, Hypervariable domain
656 of nonstructural protein nsP3 of Venezuelan equine encephalitis virus determines cell-
657 specific mode of virus replication, J Virol 87(13) (2013) 7569-84.
658 [15] Y. Gao, N. Goonawardane, J. Ward, A. Tuplin, M. Harris, Multiple roles of the non-
659 structural protein 3 (nsP3) alphavirus unique domain (AUD) during Chikungunya virus
660 genome replication and transcription, PLoS Pathog 15(1) (2019) e1007239.
661 [16] T.E. Dever, Gene-specific regulation by general translation factors, Cell 108(4) (2002)
662 545-56.
663 [17] H.P. Harding, M. Calfon, F. Urano, I. Novoa, D. Ron, Transcriptional and translational
664 control in the Mammalian unfolded protein response, Annu Rev Cell Dev Biol 18 (2002)
665 575-99.
666 [18] E. McEwen, N. Kedersha, B. Song, D. Scheuner, N. Gilks, A. Han, J.J. Chen, P.
667 Anderson, R.J. Kaufman, Heme-regulated inhibitor kinase-mediated phosphorylation of
668 eukaryotic translation initiation factor 2 inhibits translation, induces stress granule
669 formation, and mediates survival upon arsenite exposure, J Biol Chem 280(17) (2005)
670 16925-33.
671 [19] S.A. Wek, S. Zhu, R.C. Wek, The histidyl-tRNA synthetase-related sequence in the
672 eIF-2 alpha protein kinase GCN2 interacts with tRNA and is required for activation in
673 response to starvation for different amino acids, Mol Cell Biol 15(8) (1995) 4497-506.

674 [20] M.A. Garcia, E.F. Meurs, M. Esteban, The dsRNA protein kinase PKR: virus and cell
675 control, Biochimie 89(6-7) (2007) 799-811.
676 [21] H.P. Harding, Y. Zhang, A. Bertolotti, H. Zeng, D. Ron, Perk is essential for
677 translational regulation and cell survival during the unfolded protein response, Mol Cell
678 5(5) (2000) 897-904.
679 [22] I. Ventoso, M.A. Sanz, S. Molina, J.J. Berlanga, L. Carrasco, M. Esteban,
680 Translational resistance of late alphavirus mRNA to eIF2alpha phosphorylation: a
681 strategy to overcome the antiviral effect of protein kinase PKR, Genes Dev 20(1) (2006)
682 87-100.
683 [23] R. Toribio, I. Diaz-Lopez, J. Boskovic, I. Ventoso, An RNA trapping mechanism in
684 Alphavirus mRNA promotes ribosome stalling and translation initiation, Nucleic Acids Res
685 44(9) (2016) 4368-80.
686 [24] A.P. Rathore, M.L. Ng, S.G. Vasudevan, Differential unfolded protein response
687 during Chikungunya and Sindbis virus infection: CHIKV nsP4 suppresses eIF2alpha
688 phosphorylation, Virol J 10 (2013) 36.
689 [25] N. Kedersha, P. Anderson, Mammalian stress granules and processing bodies,
690 Methods Enzymol 431 (2007) 61-81.
691 [26] N. Kedersha, M.D. Panas, C.A. Achorn, S. Lyons, S. Tisdale, T. Hickman, M. Thomas,
692 J. Lieberman, G.M. McInerney, P. Ivanov, P. Anderson, G3BP-Caprin1-USP10
693 complexes mediate stress granule condensation and associate with 40S subunits, J Cell
694 Biol 212(7) (2016) 845-60.
695 [27] H. Matsuki, M. Takahashi, M. Higuchi, G.N. Makokha, M. Oie, M. Fujii, Both G3BP1
696 and G3BP2 contribute to stress granule formation, Genes Cells 18(2) (2013) 135-46.

697 [28] J.J. Fros, G.P. Pijlman, Alphavirus Infection: Host Cell Shut-Off and Inhibition of
698 Antiviral Responses, Viruses 8(6) (2016).
699 [29] J.R. Wheeler, T. Matheny, S. Jain, R. Abrisch, R. Parker, Distinct stages in stress
700 granule assembly and disassembly, Elife 5 (2016).
701 [30] N. Kedersha, G. Stoecklin, M. Ayodele, P. Yacono, J. Lykke-Andersen, M.J. Fritzler,
702 D. Scheuner, R.J. Kaufman, D.E. Golan, P. Anderson, Stress granules and processing
703 bodies are dynamically linked sites of mRNP remodeling, J Cell Biol 169(6) (2005) 871-
704 84.
705 [31] N. Kedersha, M.R. Cho, W. Li, P.W. Yacono, S. Chen, N. Gilks, D.E. Golan, P.
706 Anderson, Dynamic shuttling of TIA-1 accompanies the recruitment of mRNA to
707 mammalian stress granules, J Cell Biol 151(6) (2000) 1257-68.
708 [32] J.J. Fros, N.E. Domeradzka, J. Baggen, C. Geertsema, J. Flipse, J.M. Vlak, G.P.
709 Pijlman, Chikungunya virus nsP3 blocks stress granule assembly by recruitment of G3BP
710 into cytoplasmic foci, J Virol 86(19) (2012) 10873-9.
711 [33] A.K. Jayabalan, S. Adivarahan, A. Koppula, R. Abraham, M. Batish, D. Zenklusen,
712 D.E. Griffin, A.K.L. Leung, Stress granule formation, disassembly, and composition are
713 regulated by alphavirus ADP-ribosylhydrolase activity, Proc Natl Acad Sci U S A 118(6)
714 (2021) e2021719118.
715 [34] G. Shin, S.A. Yost, M.T. Miller, E.J. Elrod, A. Grakoui, J. Marcotrigiano, Structural
716 and functional insights into alphavirus polyprotein processing and pathogenesis, Proc
717 Natl Acad Sci U S A 109(41) (2012) 16534-9.

718 [35] L. Pohjala, A. Utt, M. Varjak, A. Lulla, A. Merits, T. Ahola, P. Tammela, Inhibitors of
719 alphavirus entry and replication identified with a stable Chikungunya replicon cell line and
720 virus-based assays, PLoS One 6(12) (2011) e28923.
721 [36] K. Tsetsarkin, S. Higgs, C.E. McGee, X. De Lamballerie, R.N. Charrel, D.L.
722 Vanlandingham, Infectious clones of Chikungunya virus (La Reunion isolate) for vector
723 competence studies, Vector Borne Zoonotic Dis 6(4) (2006) 325-37.
724 [37] G.C. Roberts, C. Zothner, R. Remenyi, A. Merits, N.J. Stonehouse, M. Harris,
725 Evaluation of a range of mammalian and mosquito cell lines for use in Chikungunya virus
726 research, Sci Rep 7(1) (2017) 14641.
727 [38] E.M. Morazzani, M.R. Wiley, M.G. Murreddu, Z.N. Adelman, K.M. Myles, Production
728 of virus-derived ping-pong-dependent piRNA-like small RNAs in the mosquito soma,
729 PLoS Pathog 8(1) (2012) e1002470.
730 [39] R. Sumpter, Jr., Y.M. Loo, E. Foy, K. Li, M. Yoneyama, T. Fujita, S.M. Lemon, M.
731 Gale, Jr., Regulating intracellular antiviral defense and permissiveness to hepatitis C virus
732 RNA replication through a cellular RNA helicase, RIG-I, J Virol 79(5) (2005) 2689-99.
733 [40] G.C. Roberts, N.J. Stonehouse, M. Harris, The Chikungunya virus nsP3 macro
734 domain inhibits activation of the NF-κB pathway, bioRxiv (2019) doi:
735 https://doi.org/10.1101/756320.
736 [41] G.F. Zhu, Z.H. Liu, J. Wang, Improved technic for dengue virus micro cell culture,
737 Chin Med J (Engl) 97(1) (1984) 73-4.
738 [42] M. Mehrabi, S. Hosseinkhani, S. Ghobadi, Stabilization of firefly luciferase against
739 thermal stress by osmolytes, Int J Biol Macromol 43(2) (2008) 187-91.

740 [43] W.C. Lane, M.D. Dunn, C.L. Gardner, L.K.M. Lam, A.M. Watson, A.L. Hartman, K.D.
741 Ryman, W.B. Klimstra, The Efficacy of the Interferon Alpha/Beta Response versus
742 Arboviruses Is Temperature Dependent, mBio 9(2) (2018).
743 [44] V.H. Leonard, A. Kohl, T.J. Hart, R.M. Elliott, Interaction of Bunyamwera
744 Orthobunyavirus NSs protein with mediator protein MED8: a mechanism for inhibiting the
745 interferon response, J Virol 80(19) (2006) 9667-75.
746 [45] R.W. Malone, J. Homan, M.V. Callahan, J. Glasspool-Malone, L. Damodaran, B.
747 Schneider Ade, R. Zimler, J. Talton, R.R. Cobb, I. Ruzic, J. Smith-Gagen, D. Janies, J.
748 Wilson, G. Zika Response Working, Zika Virus: Medical Countermeasure Development
749 Challenges, PLoS Negl Trop Dis 10(3) (2016) e0004530.
750 [46] F. Weber, E.F. Dunn, A. Bridgen, R.M. Elliott, The Bunyamwera virus nonstructural
751 protein NSs inhibits viral RNA synthesis in a minireplicon system, Virology 281(1) (2001)
752 67-74.
753 [47] M. Mutso, S. Saul, K. Rausalu, O. Susova, E. Zusinaite, S. Mahalingam, A. Merits,
754 Reverse genetic system, genetically stable reporter viruses and packaged subgenomic
755 replicon based on a Brazilian Zika virus isolate, J Gen Virol 98(11) (2017) 2712-2724.
756 [48] J. Saraste, L. Kaaiainen, H. Soderlund, S. Keranen, RNA synthesis directed by a
757 temperature-sensitive mutant of Semliki Forest virus, J Gen Virol 37(2) (1977) 399-406.
758 [49] L. Kaariainen, D. Sawicki, P.J. Gomatos, Cleavage defect in the non-structural
759 polyprotein of Semliki Forest virus has two separate effects on virus RNA synthesis, J
760 Gen Virol 39(3) (1978) 463-73.
761 [50] J. Suopanki, D.L. Sawicki, S.G. Sawicki, L. Kaariainen, Regulation of alphavirus 26S
762 mRNA transcription by replicase component nsP2, J Gen Virol 79 (Pt 2) (1998) 309-19.

763 [51] C. Sidrauski, D. Acosta-Alvear, A. Khoutorsky, P. Vedantham, B.R. Hearn, H. Li, K.
764 Gamache, C.M. Gallagher, K.K. Ang, C. Wilson, V. Okreglak, A. Ashkenazi, B. Hann, K.
765 Nader, M.R. Arkin, A.R. Renslo, N. Sonenberg, P. Walter, Pharmacological brake-release
766 of mRNA translation enhances cognitive memory, Elife 2 (2013) e00498.
767 [52] C. Sidrauski, A.M. McGeachy, N.T. Ingolia, P. Walter, The small molecule ISRIB
768 reverses the effects of eIF2alpha phosphorylation on translation and stress granule
769 assembly, Elife 4 (2015).
770 [53] P. Anderson, N. Kedersha, RNA granules: post-transcriptional and epigenetic
771 modulators of gene expression, Nat Rev Mol Cell Biol 10(6) (2009) 430-6.
772 [54] C.L. Miller, Stress Granules and Virus Replication, Future Virol 6(11) (2011) 1329-
773 1338.
774 [55] F.E. Scholte, A. Tas, I.C. Albulescu, E. Zusinaite, A. Merits, E.J. Snijder, M.J. van
775 Hemert, Stress granule components G3BP1 and G3BP2 play a proviral role early in
776 Chikungunya virus replication, J Virol 89(8) (2015) 4457-69.
777 [56] Y. Suzuki, M. Minami, M. Suzuki, K. Abe, S. Zenno, M. Tsujimoto, K. Matsumoto, Y.
778 Minami, The Hsp90 inhibitor geldanamycin abrogates colocalization of eIF4E and eIF4E-
779 transporter into stress granules and association of eIF4E with eIF4G, J Biol Chem 284(51)
780 (2009) 35597-604.
781 [57] Y.S. Hahn, A. Grakoui, C.M. Rice, E.G. Strauss, J.H. Strauss, Mapping of RNA-
782 temperature-sensitive mutants of Sindbis virus: complementation group F mutants have
783 lesions in nsP4, J Virol 63(3) (1989) 1194-202.
784 [58] N.A. Prow, B. Tang, J. Gardner, T.T. Le, A. Taylor, Y.S. Poo, E. Nakayama, T.D.C.
785 Hirata, H.I. Nakaya, A. Slonchak, P. Mukhopadhyay, S. Mahalingam, W.A. Schroder, W.

786 Klimstra, A. Suhrbier, Lower temperatures reduce type I interferon activity and promote
787 alphaviral arthritis, PLoS Pathog 13(12) (2017) e1006788.

788 # Figure legends

789 **Figure 1. (A) Structure of the CHIKV genome and nsP3.** The positive-sense RNA is
790 capped and polyadenylated and templates translation of the 5′ORF into the four non-
791 structural (ns) proteins which transcribe a negative-sense intermediate. Transcription of
792 a sub-genomic RNA is then initiated from the sg-prom and acts as a template for
793 translation of the 3′ORF encoding the structural proteins. nsP3 comprises 3 domains:
794 Macro-domain, AUD (alphavirus unique domain), HVD (hypervariable domain). The
795 structure of the CHIKV-Dluc subgenomic replicon (SGR) is shown. R-Luc (Renilla
796 luciferase) is expressed as a fusion within nsP3, FF-Luc (firefly luciferase) is expressed
797 from the sg-prom. **B. Three-dimensional structure of the SINV AUD [34].** Surface
798 exposed and conserved residues targeted for mutagenesis are highlighted in the
799 corresponding colours.

800 **Figure 2. Replication of CHIKV AUD mutants in mammalian and mosquito cells.**
801 C2C12 (**A**), C6/36 and U4.4 (**B**), RD, Huh7, Huh7.5 and BHK-21 cells (**D**) were
802 transfected with wildtype (WT) and mutant SGR-D-Luc and cells were harvested at
803 indicated time points. FF-Luc activities of WT and mutants were measured and
804 normalized to their respective 4 h values and thus represent fold-change compared to
805 those 4 h values. (GAA: nsP4 polymerase inactive mutant). Significant differences
806 denoted by ** ($P<0.01$), *** ($P<0.001$), **** ($P<0.0001$), compared to WT are only shown
807 for the 12 h time point for clarity. Data are displayed as the means ±S.E. of three

808 experimental replicates. (**C**) RT-PCR and sequence analysis of SGR-D-Luc W220A,
809 D249A and Y324A in U4.4 and C6/36 cells. RNAs of AUD mutants were extracted 72 h
810 post transfection (h.p.t.), followed by RT-PCR and sequence analysis.

811 **Figure 3. Replication and translation of CHIKV AUD mutants in mammalian cells at**
812 **28°C or 37°C.** C2C12 (**A**), Huh7 (**C**) and Vero cells (**D**) were transfected with WT and
813 mutant SGR-D-Luc RNAs and cultured at 28°C or 37°C. Cells were harvested at indicated
814 time points. FF-Luc activities of WT and mutants in C2C12 and Huh7 cells were measured
815 and normalized to their respective 4 h values and value represent fold-change compared
816 to the 4 h values. FF-Luc activities in Vero cells were normalized to 4 h R-Luc activities.
817 (GAA: nsP4 polymerase inactive mutant). Significant differences denoted by ** (P<0.01),
818 *** (P<0.001) **** (P<0.0001), compared to WT are only shown for the 12 h time point for
819 clarity. Data are displayed as the means ±S.E. of three experimental replicates. (**B**)
820 Protein expression of nsP1 for the WT and mutant SGR-D-Luc at 28°C or 37°C. Cells
821 were lysed at 24 h.p.t., 10 µg of each sample was loaded and analysed by western blot.
822 Actin was also detected by western blot as a loading control.

823 **Figure 4. Replication of CHIKV SGRs, Bunyamwera (BUNV) mini-genome and Zika**
824 **virus SGR at 28°C or 37°C.** (**A**) Schematic of three CHIKV SGRs. CHIKV-nsP3-
825 mCherry-FF-Luc-SGR was constructed in which the R-Luc reporter was replaced with
826 mCherry. CHIKV-FF-Luc-SGR was constructed by deleting R-Luc and thus expressing
827 WT unfused nsP3. C2C12 (**B**), Huh7 **(C)** and Vero **(D)** cells were transfected with the
828 three CHIKV SGRs and incubated at 28°C or 37°C. Cells were harvested at indicated
829 time points. FF-Luc activities of WT and mutants were measured and normalized to their
830 respective 4 h values and thus represent fold-change compared to those 4 h values (GAA:

831 nsP4 polymerase inactive mutant). Significant differences denoted by ns (P>0.05), *
832 (P<0.05), ** (P<0.01), *** (P<0.001) **** (P<0.0001), are only shown for the 12 h time
833 point for clarity. Data are displayed as the means ±S.E. of three experimental replicates.
834 Replication of BUNV mini-genome (**E**) and Zika virus SGR **(F)** at 28°C or 37°C. Cells were
835 collected at indicated time points and R-Luc or Nano luciferase (N-Luc) activities were
836 measured and normalized to their respective 4 h values.

837 **Figure 5. Phenotype of WT and AUD mutants in the context of ICRES-CHIKV and**
838 **ONNV at 28°C or 37°C.** (**A**) Phenotype of WT and AUD mutants in ICRES-CHIKV
839 production at 28°C or 37°C. C2C12 cells were transfected with WT and mutant ICRES-
840 CHIKV RNA and incubated at 28°C or 37°C. Supernatants were collected 48 h post
841 infection (h.p.i.) from both temperatures and titrated at 37°C by plaque assay. (**B**)
842 Schematic of ONNV-2SG-ZsGreen. ZsGreen was inserted after nsP4 and expressed by
843 a duplicated sub-genomic promoter (sg-prom). (**C**) Normalized ZsGreen expression of
844 WT and mutant ONNV at 48 h.p.t at 28°C or 37°C. C2C12 cells were transfected with WT
845 and mutant ONNV RNAs and incubated at 28°C or 37°C. Cells were fixed with 4%
846 formaldehyde at 48 h.p.t. and ZsGreen expression were scanned and normalized by
847 EVOS microscopy. *** (P<0.001) **** (P<0.0001), compared to WT at their respective
848 temperature. Data are displayed as the means ±S.E. of three experimental replicates. (**D**)
849 Virus production of WT and mutant ONNV harvested from 28°C or 37°C. Supernatants of
850 WT and mutant ONNV collected from cells at 28°C or 37°C at 48 h.p.i were titrated by
851 plaque assay on BHK-21 cells at 37°C or 28°C. BHK-21 cells were fixed with 4%
852 formaldehyde at 72 h.p.i at 37°C or at 96 h.p.i at 28°C. Infectivity was determined by
853 enumerating ZsGreen-positive cells using EVOS microscopy.

854 **Figure 6. Temperature shift assay of WT SGR-D-Luc.** (**A**) Schematic of temperature
855 shift assay. Transfected cells were incubated at either 28°C or 37°C prior to a temperature
856 shift from 12-24 h.p.t. (28°C to 37°C (designated 24 h S#) and 37°C to 28°C (designated
857 24 h S*) respectively). Controls maintained the same temperature from 0-24 h.p.t. (**B**)
858 Replication of WT SGR-D-Luc at 28°C or 37°C. WT SGR-D-Luc RNA was transfected
859 into C2C12 cells and incubated at 28°C or 37°C according to the schematic in (A) FF-Luc
860 activities were measured and normalized to their respective 4 h values. Significant
861 differences denoted by ** (P<0.01), **** (P<0.0001), compared to replication at 12 h.p.t.
862 Data are displayed as the means ±S.E. of three experimental replicates. Cell numbers
863 were enumerated (**C**) and cell metabolic activity **(D)** determined by MTT assay at 28°C or
864 37°C. **(E)** Protein expression of nsP1 at 28°C or 37°C. Cells were lysed at 24 h.p.t. and
865 10 µg of each sample was analysed by western blot. Actin was also detected by western
866 blot as a loading control.

867 **Figure 7. ISRIB treatment did not recover the replication phenotype of AUD mutants.**
868 (**A**) Replication of SGR-D-Luc W220A was not recovered by ISRIB treatment at 37°C.
869 C2C12 cells were transfected with SGR-D-Luc WT or W220A RNA and incubated at 28°C
870 or 37°C. Cells were then harvested at indicated time points. FF-Luc activities were
871 measured and normalized to their respective 4 h values and thus represent fold-change
872 compared to those 4 h values (GAA: nsP4 polymerase inactive mutant). Significant
873 differences denoted by ns (P>0.05), ** (P<0.01), compared to replication at 24 h.p.t.
874 without ISRIB at the respective temperatures. Data are displayed as the means ±S.E. of
875 three experimental replicates. (**B**) Replication of ONNV W220A was not recovered by
876 ISRIB at 37°C. C2C12 cells were infected with ONNV WT and W220A at MOI 0.1 and

877 incubated at 28°C or 37°C. Cells were fixed at 48 h.p.i. and ZsGreen intensities were
878 quantified by EVOS microscopy. Significant differences denoted by ** (P<0.01), ***
879 (P<0.001), **** (P<0.0001), compared to replication 48 h.p.i. without ISRIB at the
880 respective temperatures.

881 **Figure 8. Stress granule (SG) formation in uninfected cells at 28°C or 37°C.** (**A**) RD
882 cells were incubated at 28°C or 37°C. Cells were either mock treated or treated with 0.5
883 mM sodium arsenite ($NaAsO_2$) for 1 h. Cells were either fixed by 4% paraformaldehyde
884 or treated with 100 µg/ml cycloheximide (CHX) (on cells treated with $NaAsO_2$) for 45 min
885 prior to fixation. Cells were then stained with G3BP antibody (red). (**B**) Quantification of
886 G3BP protein expression from mock, $NaAsO_2$ and $NaAsO_2$ + CHX treated cells at different
887 temperatures. Values were determined for 10 cells and calculated by Fiji ImageJ**. (C)**
888 The number of SG were determined for 10 cells.

889 **Figure 9. Different sizes and numbers of SG induced by $NaAsO_2$ and ONNV at 28°C**
890 **or 37°C.** (**A**) RD cells were mock infected or infected with ONNV WT at MOI 5 and
891 incubated at 28°C or 37°C. 7 h later, mock infected cells were then treated with 0.5 mM
892 $NaAsO_2$ for 1 h. Cells were either fixed with 4% paraformaldehyde or treated with 100
893 µg/ml CHX (on cells treated with $NaAsO_2$) for 45 min prior to fixation. Cells were then
894 stained with G3BP1 antibody (red) or dsRNA antibody J2 (gray). Scale bar 1 µm. (**B**)
895 Quantification of the sizes of SG induced by $NaAsO_2$ and virus at 28°C or 37°C. The
896 sizes of SG were determined for 10 cells and calculated by Fiji ImageJ. Significant
897 differences denoted by **** (P<0.0001), compared with the sizes of virus-induced SG at
898 37°C. (**C**) Quantification of the overall dsRNA, G3BP1, ZsGreen and dsRNA/ZsGreen
899 levels at 28°C or 37°C. Values were determined for 10 cells and calculated by Fiji ImageJ.

900 Significant differences denoted by ** (P<0.01), **** (P<0.0001), compared their respective
901 protein expression at 37°C.

902 **Figure 10. TIA-1 but not eIF4G is a component of virus-induced SG at both 28°C**
903 **and 37°C.** RD cells were either mock infected **(A)** or infected with ONNV WT **(B)** at MOI
904 5 and incubated at 28°C or 37°C. 7 h later, mock infected cells were treated with 0.5 mM
905 $NaAsO_2$ for 1 h. Cells were fixed with 4% paraformaldehyde and stained with TIA-1
906 antibody, eIF4G antibody (red) or dsRNA antibody J2 (gray) as indicated .

907 # Supporting information

908 **S1 Figure.** (**A**) Sequence alignment of AUD from multiple alphaviruses indicating key
909 mutated residues. (**B**) Ribbon structure of SINV AUD (PDB ID code 4GUA) with the
910 mutants shown in different colors [34]. Image was constructed using PyMol.

911 **S2 Figure. R-Luc activities of WT and mutant SGR-D-Luc in mammalian cells at**
912 **28°C or 37°C.** The detailed transfection procedure was shown in Figure 3. R-Luc activities
913 of WT and mutant SGR-D-Luc were measured and normalized to their respective 4 h
914 values and thus represent fold-change compared to their respective 4 h values. (GAA:
915 nsP4 polymerase inactive mutant).

916 **S3 Figure. ISRIB titration.** (**A**) Replication of WT SGR-D-Luc with different
917 concentrations of ISRIB. C2C12 cells were transfected with WT SGR-D-Luc and
918 incubated at 28°C or 37°C. Different concentrations of ISRIB were added 2 h.p.t at 37°C.
919 Cells were harvested at indicated time points and FLuc activities were measured. (**B**) Cell
920 viability of different concentrations of ISRIB by MTT assay. Along with the transfection,

921 different concentrations of ISRIB were added to mock transfected cells, followed by MTT
922 assay.

923 **S4 Figure. Replication of WT and W220A SGR-D-Luc or ONNV with or without ISRIB**
924 **at 32°C.** (**A**) Replication of WT and W220A SGR-D-Luc with or without ISIRB at 32°C.
925 C2C12 cells were transfected with WT or W220A SGR-D-Luc RNA and incubated at 32°C.
926 Cells were treated with 200 nM ISRIB at 2 h.p.t and collected at indicated time points and
927 FF-Luc activities from each time point were normalized to their respective 4 h value. (**B**)
928 Replication of WT and W220A ONNV with or without ISRIB at 32°C. C2C12 cells were
929 infected with WT or W220A ONNV at an MOI of 0.1 and incubated at 32°C. Cells were
930 treated with 200 nM ISRIB at 0 h.p.t and were fixed by 4% paraformaldehyde at 48 h.p.i.
931 ZsGreen expression were measured by EVOS microscopy.

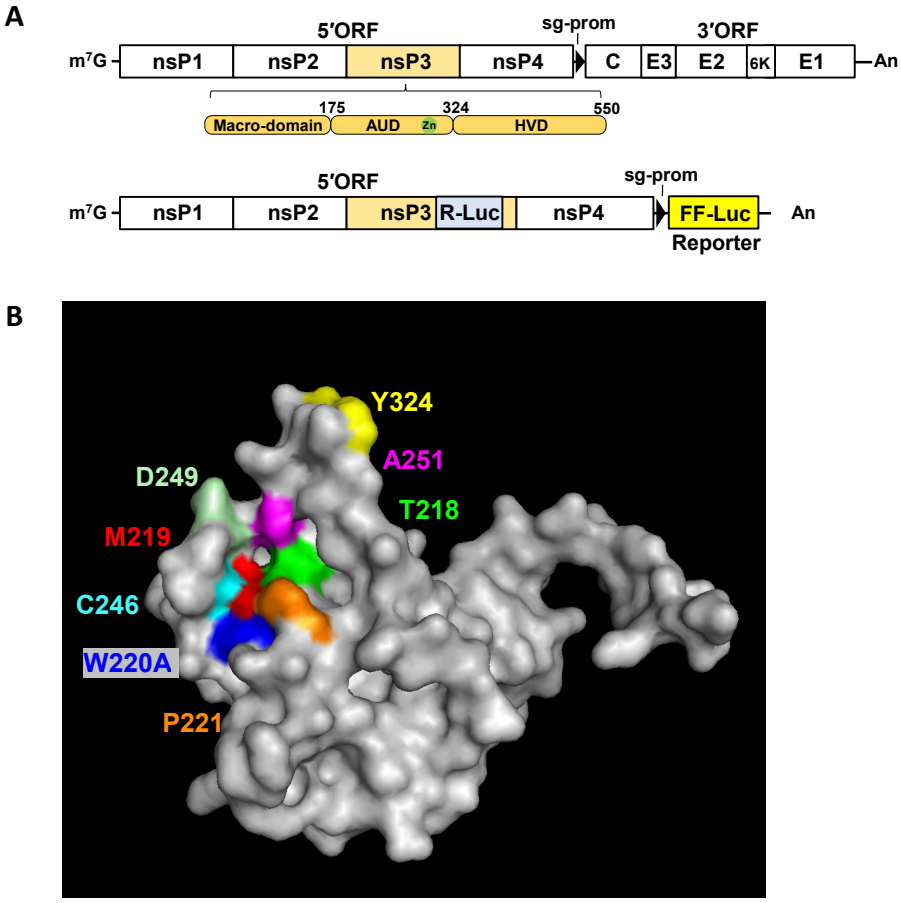
A
5′ORF
sg-prom
3′ORF
m7G
nsP1
nsP2
nsP3
nsP4
C
E3
E2
6K
E1
An
175
324
550
Macro-domain
AUD
Zn
HVD
5′ORF
sg-prom
m7G
nsP1
nsP2
nsP3
R-Luc
nsP4
FF-Luc
An
Reporter
B
Y324
A251
D249
T218
M219
C246
W220A
P221

Figure 1

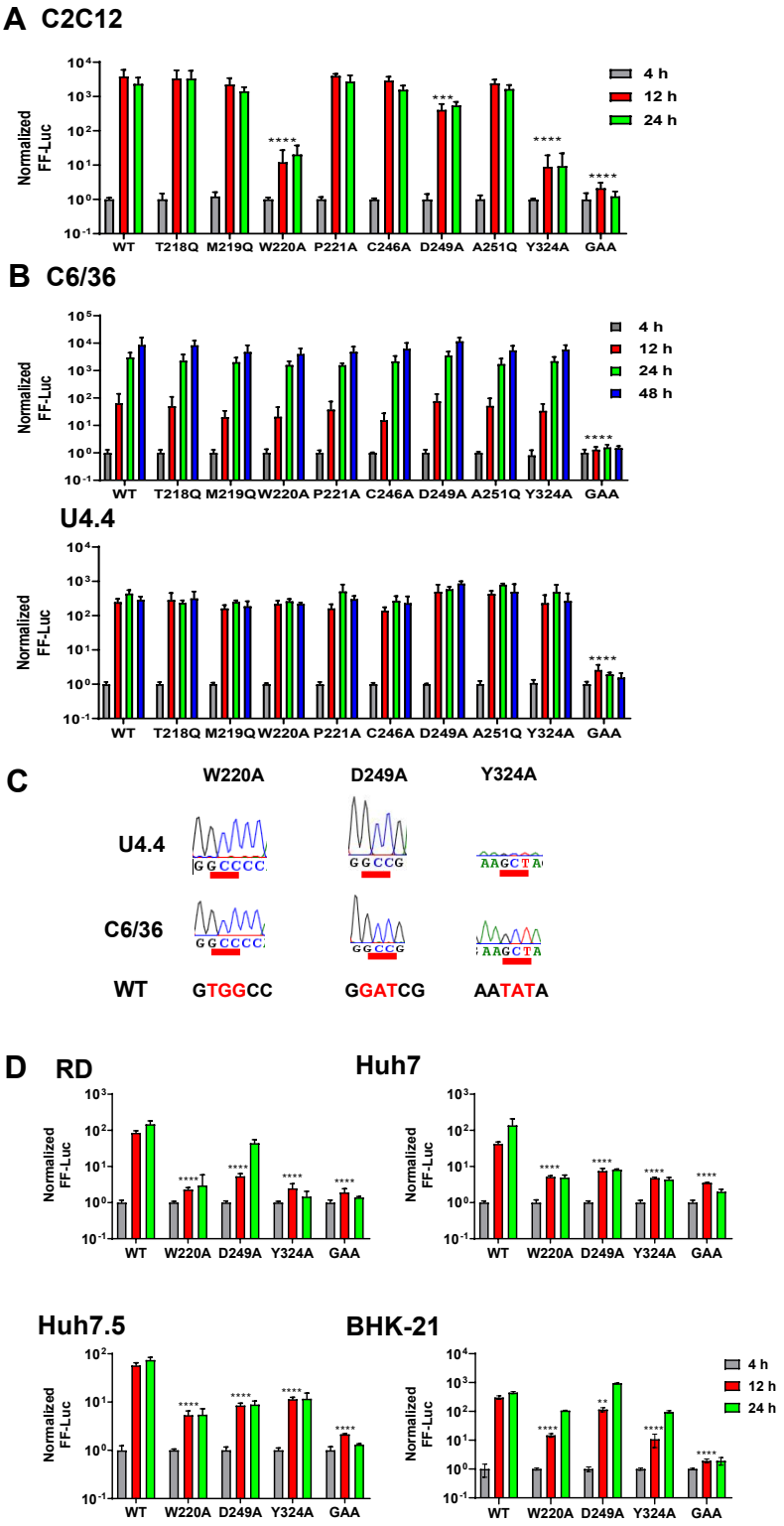
A C2C12
Normalized FF-Luc
4 h
12 h
24 h
WT T218Q M219Q W220A P221A C246A D249A A251Q Y324A GAA
B C6/36
4 h
12 h
24 h
48 h
U4.4
C
W220A
D249A
Y324A
U4.4
C6/36
WT
GTGGCC
GGATCG
AATATA
D
RD
Huh7
Huh7.5
BHK-21
WT W220A D249A Y324A GAA

Figure 2

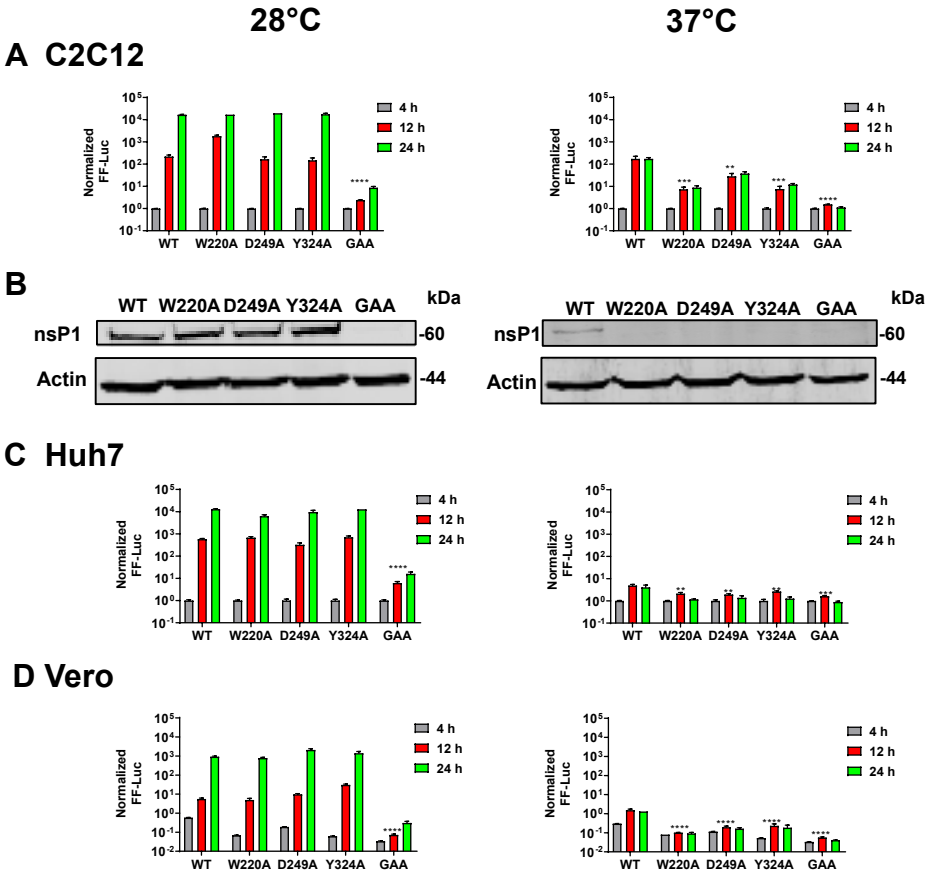
28°C
37°C
A C2C12
Normalized FF-Luc
4 h
12 h
24 h
WT
W220A
D249A
Y324A
GAA
B
kDa
nsP1
Actin
-60
-44
C Huh7
D Vero

Figure 3

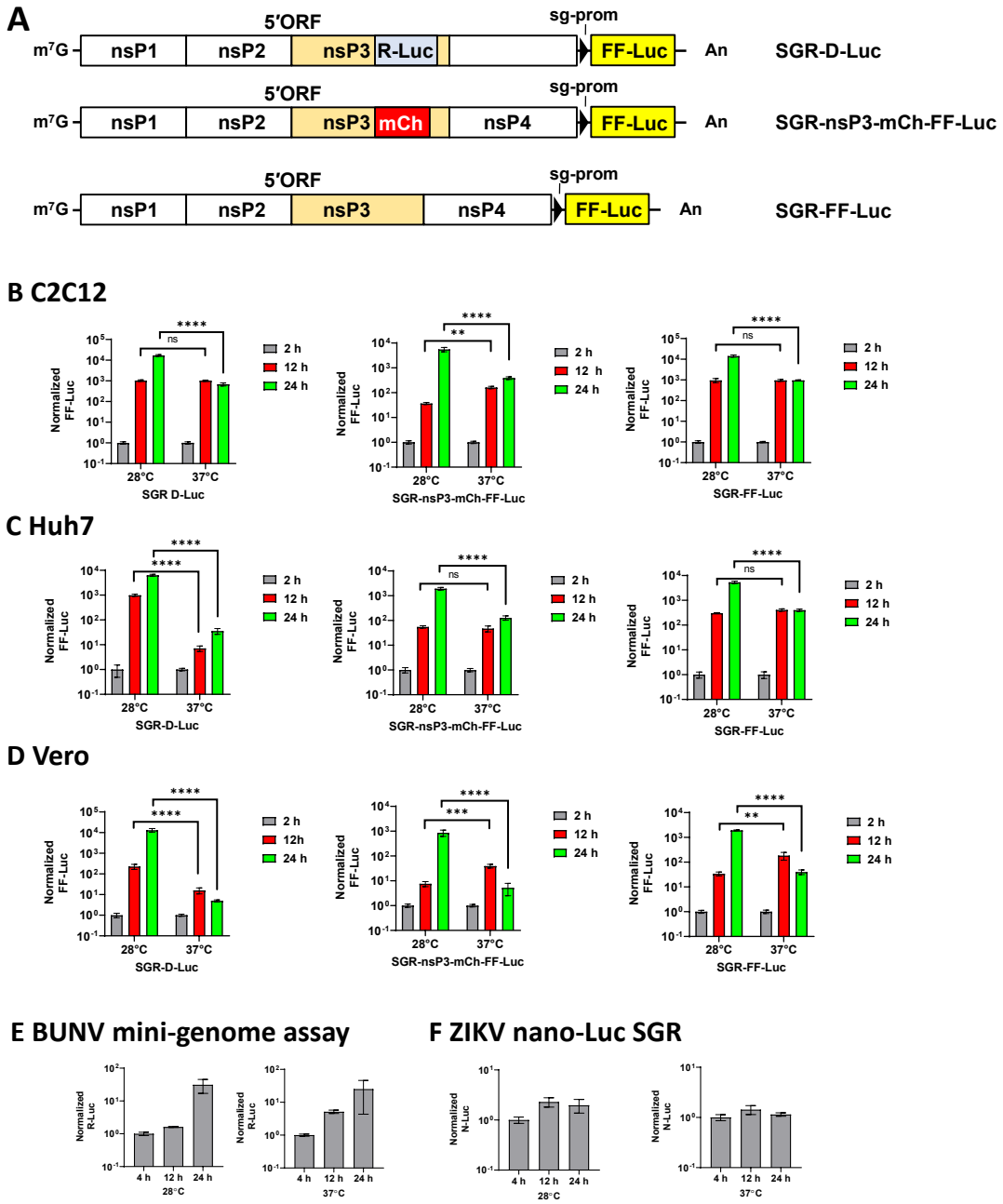
A
5'ORF
sg-prom
m7G
nsP1
nsP2
nsP3
R-Luc
FF-Luc
An
SGR-D-Luc
mCh
nsP4
SGR-nsP3-mCh-FF-Luc
SGR-FF-Luc
B C2C12
C Huh7
D Vero
Normalized FF-Luc
2 h
12 h
24 h
28°C
37°C
SGR D-Luc
SGR-D-Luc
SGR-nsP3-mCh-FF-Luc
SGR-FF-Luc
ns
E BUNV mini-genome assay
F ZIKV nano-Luc SGR
Normalized R-Luc
Normalized N-Luc
4 h
12 h
24 h

Figure 4

A ICRES CHIKV titre

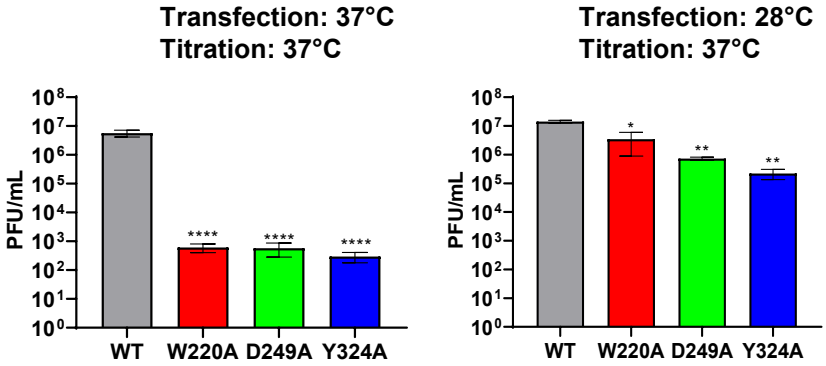

B ONNV-ZsGreen

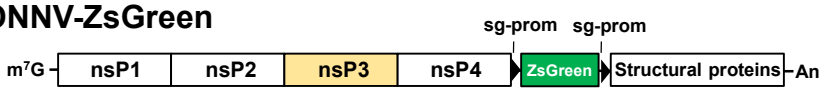

C

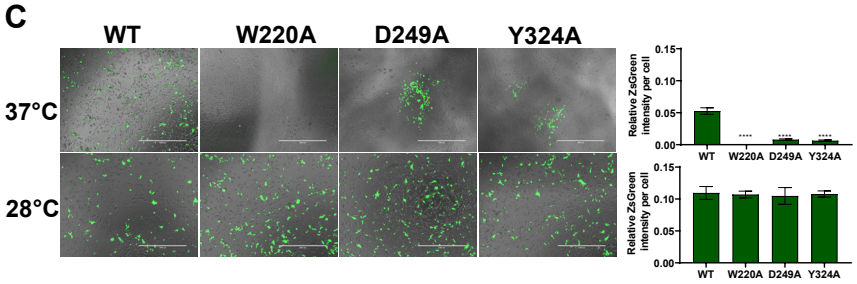

D ONNV-ZsGreen virus titre

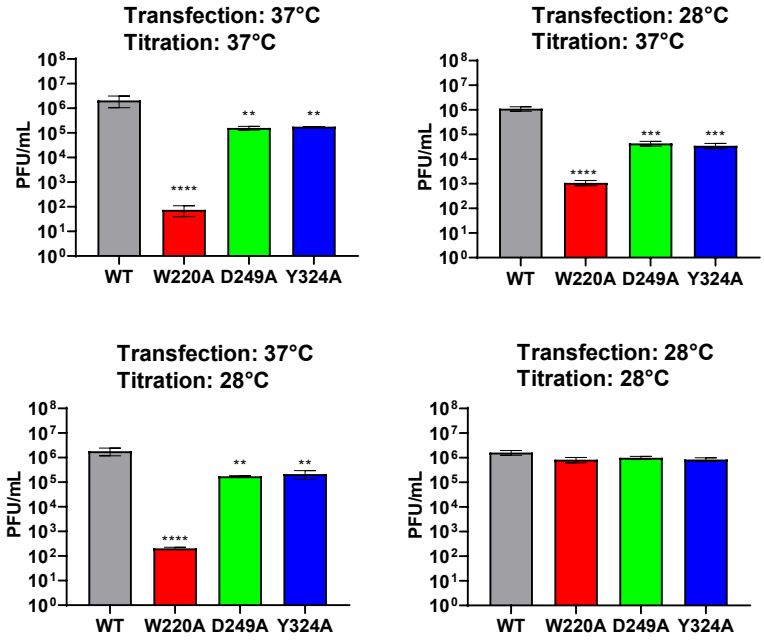

Figure 5

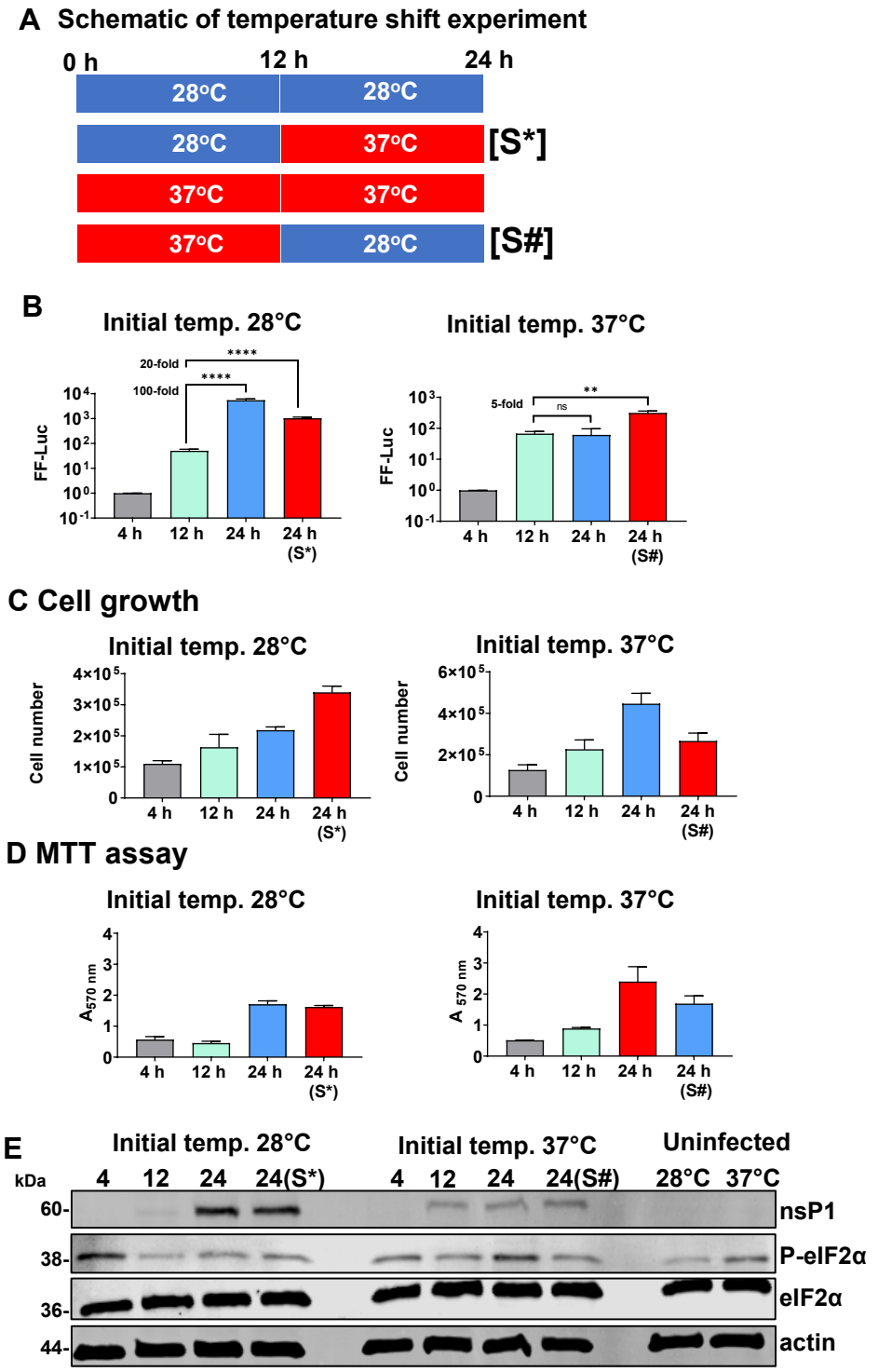
A Schematic of temperature shift experiment
0 h
12 h
24 h
28ºC
28ºC
28ºC
37ºC
[S*]
37ºC
37ºC
37ºC
28ºC
[S#]
B
Initial temp. 28°C
Initial temp. 37°C
FF-Luc
20-fold
100-fold
5-fold
ns
4 h
12 h
24 h
24 h (S*)
24 h (S#)
C Cell growth
Cell number
D MTT assay
A570 nm
E
kDa
4
12
24
24(S*)
24(S#)
28°C
37°C
Uninfected
60-
38-
36-
44-
nsP1
P-eIF2α
eIF2α
actin

Figure 6

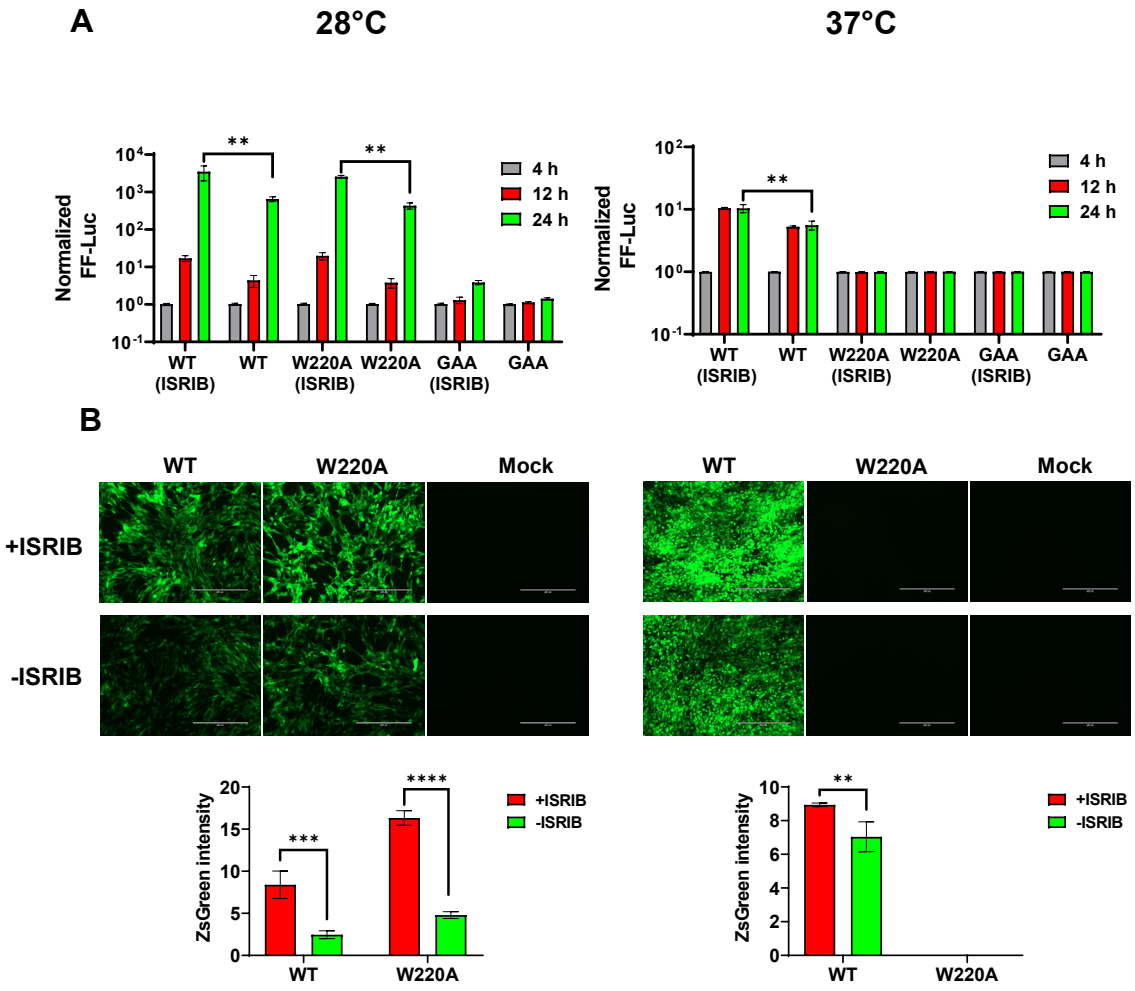
A
28°C
37°C
Normalized FF-Luc
4 h
12 h
24 h
WT (ISRIB)
WT
W220A (ISRIB)
W220A
GAA (ISRIB)
GAA
B
WT
W220A
Mock
+ISRIB
-ISRIB
ZsGreen intensity
+ISRIB
-ISRIB

Figure 7

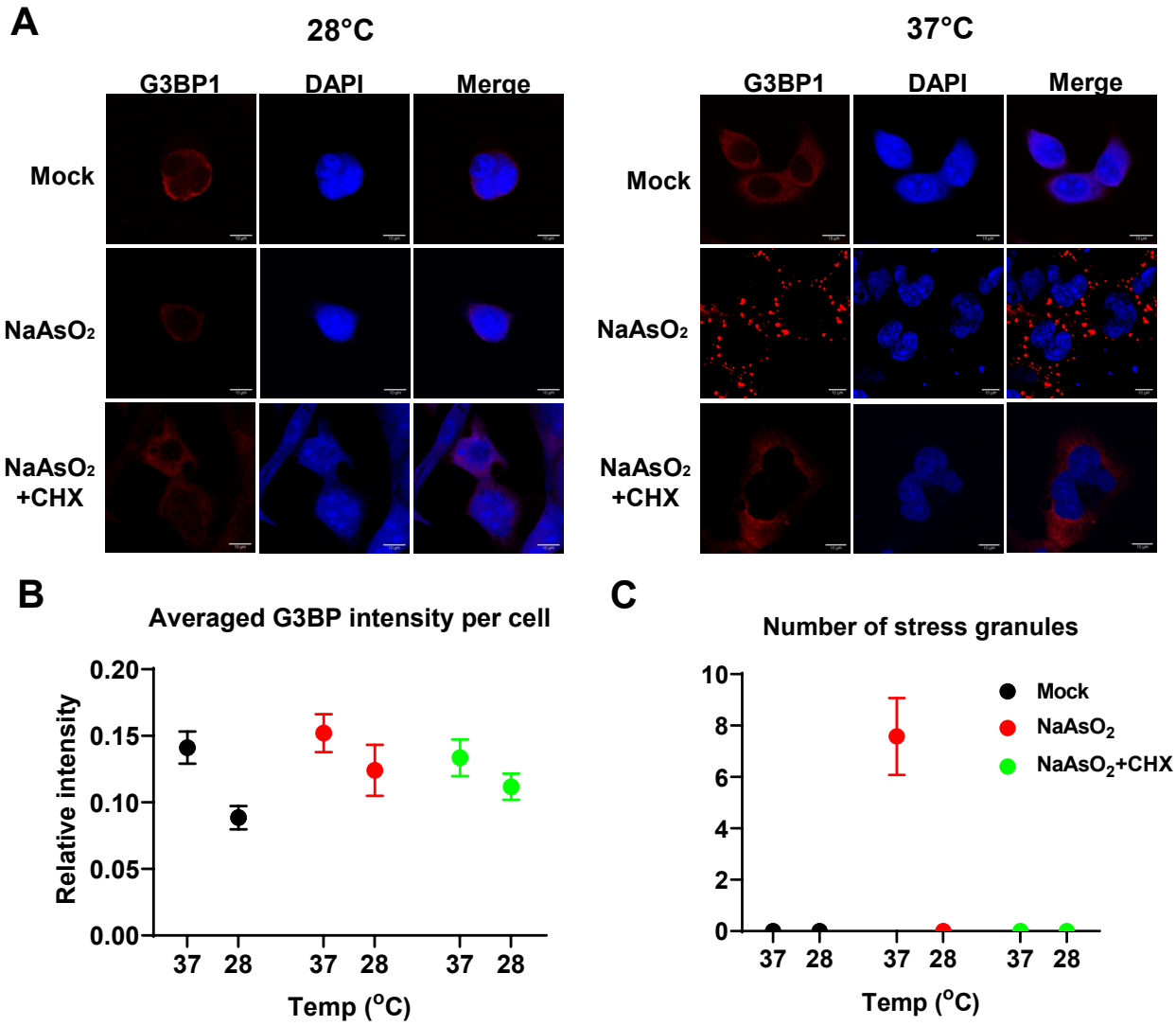
A
28°C
37°C
G3BP1
DAPI
Merge
Mock
NaAsO2
NaAsO2 +CHX
B
Averaged G3BP intensity per cell
Relative intensity
0.20
0.15
0.10
0.05
0.00
37 28 37 28 37 28
Temp (°C)
C
Number of stress granules
10
8
6
4
2
0
Mock
NaAsO2
NaAsO2+CHX
37 28 37 28 37 28
Temp (°C)

Figure 8

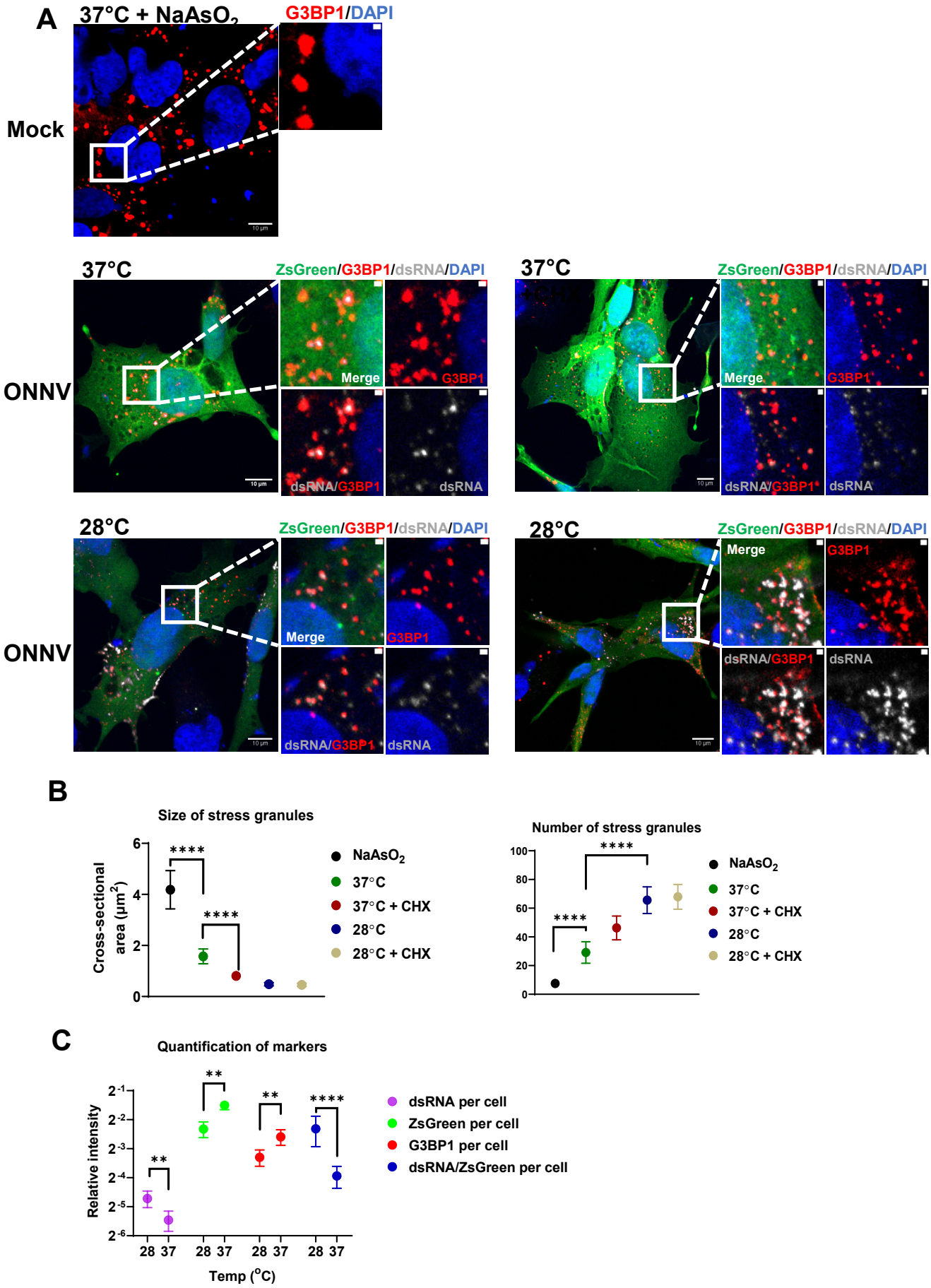
A
37°C + NaAsO2
G3BP1/DAPI
Mock
37°C
ZsGreen/G3BP1/dsRNA/DAPI
ONNV
Merge
G3BP1
dsRNA/G3BP1
dsRNA
+CHX
28°C
B
Size of stress granules
Cross-sectional area (µm2)
****
NaAsO2
37°C
37°C + CHX
28°C
28°C + CHX
Number of stress granules
C
Quantification of markers
Relative intensity
**
dsRNA per cell
ZsGreen per cell
G3BP1 per cell
dsRNA/ZsGreen per cell
28 37
Temp (°C)

Figure 9

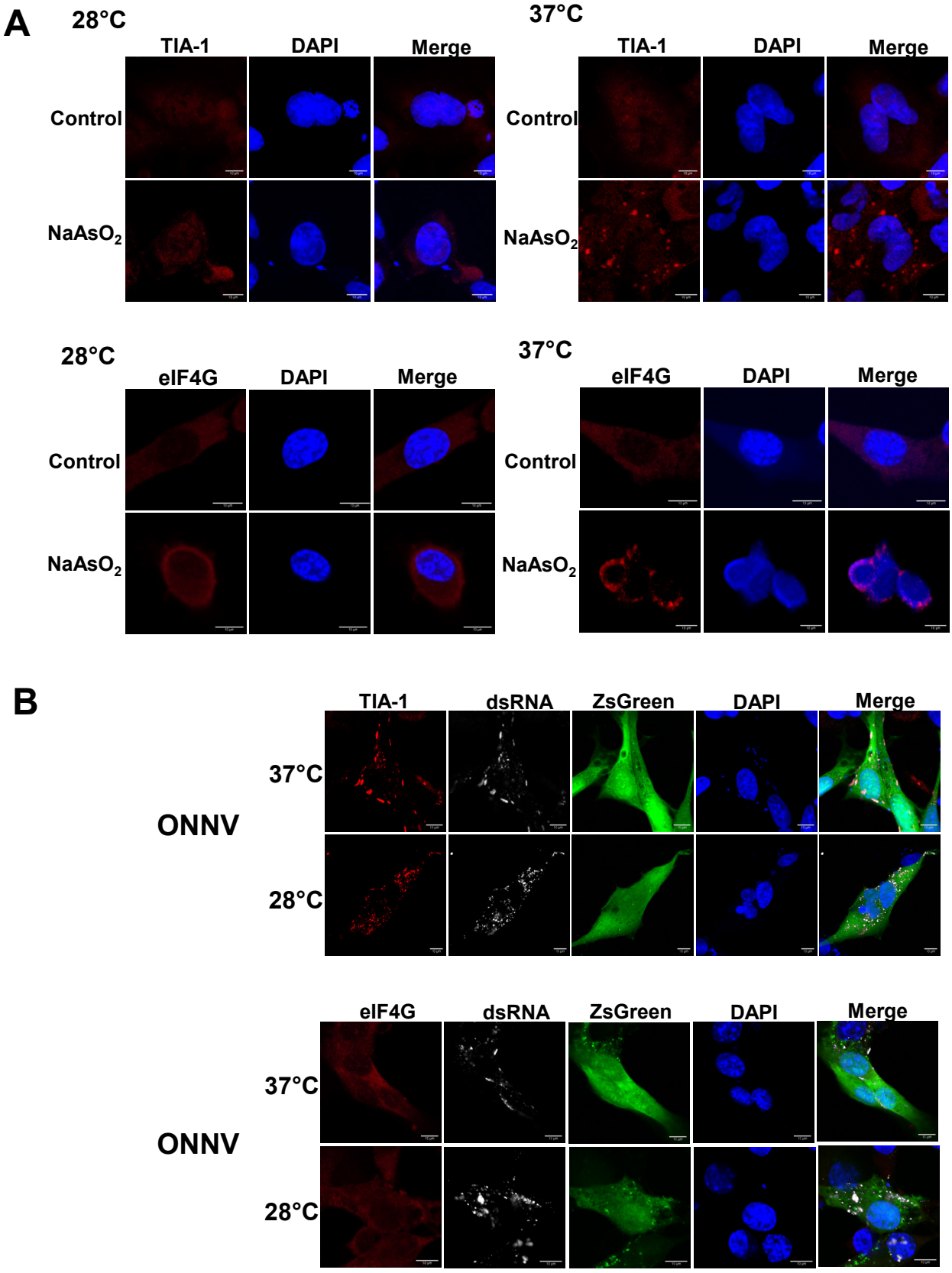
A
28°C
37°C
TIA-1
DAPI
Merge
Control
NaAsO2
eIF4G
B
ONNV
dsRNA
ZsGreen

Figure 10